Molecular Phylogenetics and Evolution 167 (2022) 107356

Contents lists available at ScienceDirect

Molecular Phylogenetics and Evolution

journal homepage: www.elsevier.com/locate/ympev

Genome-wide ultraconserved elements resolve phylogenetic relationships and biogeographic history among Neotropical leaf-nosed bats in the genus *Anoura* (Phyllostomidae)

Camilo A. Calderón-Acevedo [a,d,1,*], Justin C. Bagley [a,b,c,1], Nathan Muchhala [a]

[a] Department of Biology, University of Missouri–St. Louis, One University Blvd., 223 Research Bldg., St. Louis, MO 63121, USA
[b] Department of Biology, Jacksonville State University, 242 Martin Hall, 700 Pelham Rd North, Jacksonville, AL 36265, USA
[c] Department of Biology, Virginia Commonwealth University, 1000 W Cary St., Suite 126, Richmond, VA 23284, USA
[d] Department of Earth and Environmental Science, Rutgers University, 195 University Ave., Boyden Hall 433, Newark, NJ, 07102 USA

ARTICLE INFO

Keywords:
Incomplete lineage sorting
multispecies coalescent (MSC)
Phyllostomidae
Phylogenomics
Species trees
Ultraconserved elements

ABSTRACT

Anoura Gray, 1838 are Neotropical nectarivorous bats and the most speciose genus within the phyllostomid subfamily Glossophaginae. However, *Anoura* species limits remain debated, and phylogenetic relationships remain poorly known, because previous studies used limited *Anoura* taxon sampling or focused primarily on higher-level relationships. Here, we conduct the first phylogenomic study of *Anoura* by analyzing 2039 genome-wide ultraconserved elements (UCEs) sequenced for 42 individuals from 8 *Anoura* species/lineages plus two outgroups. Overall, our results based on UCEs resolved relationships in the genus and supported (1) the monophyly of small-bodied *Anoura* species (previously genus *Lonchoglossa*); (2) monotypic status of *A. caudifer*; and (3) nested positions of "*A. carishina*", *A. caudifer aequatoris*, and *A. geoffroyi peruana* specimens within *A. latidens*, *A. caudifer* and *A. geoffroyi*, respectively (suggesting that these taxa are not distinct species). Additionally, (4) phylogenetic networks allowing reticulate edges did not explain gene tree discordance better than the species tree (without introgression), indicating that a coalescent model accounting for discordance solely through incomplete lineage sorting fit our data well. Sensitivity analyses indicated that our species tree results were not adversely affected by varying taxon sampling across loci. Tree calibration and Bayesian coalescent analyses dated the onset of diversification within *Anoura* to around ~ 6–9 million years ago in the Miocene, with extant species diverging mainly within the past ~ 4 million years. We inferred a historical biogeographical scenario for *Anoura* of parapatric speciation fragmenting the range of a wide-ranging ancestral lineage centered in the Central to Northern Andes, along with Pliocene–Pleistocene dispersal or founder event speciation in Amazonia and the Brazilian Atlantic forest during the last ~ 2.5 million years.

1. Introduction

Anoura Gray, 1838 (NCBI:txid27641) is a genus of nectarivorous, leaf-nosed bats in the family Phyllostomidae, and is the most speciose genus within the subfamily Glossophaginae (Griffiths and Gardner, 2008; Pacheco et al., 2018; Calderón-Acevedo, 2019; Cirranello and Simmons, 2020; Calderón-Acevedo et al., 2021). Extant *Anoura* species are endemic to and widespread throughout the Neotropics, where they form important components of Andean forest ecosystems (Griffiths and Gardner, 2008; Pacheco et al., 2018; Calderón-Acevedo and Muchhala 2018, 2020) and contribute to high species richness of the Tropical Andes biodiversity 'hotspot' (Myers et al., 2000). With the exception of recently discovered and lesser-known species (e.g. *A. javieri*; Pacheco et al., 2018), *Anoura* are relatively common based on mist net surveys and are in most cases supported by large museum series (Jarrín-V. and Kunz, 2008; de Moraes Weber and Grelle, 2012). Recently, *Anoura* have garnered attention as model organisms for studying the evolutionary ecology of angiosperm pollination (e.g. Muchhala, 2006; Muchhala and Thompson, 2009) and they are considered among the most important mammalian pollinators in Andean cloud forests (e.g. Muchhala and Jarrín-V., 2002; Jarrín-V. and Kunz, 2008). However, our knowledge of the evolutionary origins, classification, trait evolution, and

* Corresponding author at: Department of Earth and Environmental Science, Rutgers University, 195 University Ave., Boyden Hall 433, Newark, NJ, 07102 USA
E-mail addresses: camilo.calderon@rutgers.edu (C.A. Calderón-Acevedo), jbagley@jsu.edu (J.C. Bagley), muchhalan@umsl.edu (N. Muchhala).
[1] These lead authors contributed equally to this work.

https://doi.org/10.1016/j.ympev.2021.107356
Received 12 July 2021; Received in revised form 26 October 2021; Accepted 8 November 2021
Available online 10 November 2021

biogeography of *Anoura* bats has been impeded by taxonomic instability, including disagreements over species status, as well as lack of a well-resolved hypothesis of species phylogenetic relationships.

Over 180 years ago, Gray (1838) described *Anoura* as a monotypic genus from a single *A. geoffroyi* specimen. Since then, the taxonomy of the genus has "suffered a long and tortuous history" (Jarrín-V. and Kunz, 2008), in part owing to the fact that *Anoura* exhibit a wide degree of overlap in external anatomical characteristics. Still, *Anoura* exhibit two well-known patterns of morphological variation. First, the genus contains the mammal species with the longest tongue relative to body size, *A. fistulata*, which can extend its tongue to 8.5 cm versus only 3–5 cm for other *Anoura* (Muchhala, 2006; Calderón-Acevedo and Muchhala, 2018). Second, there is divergence in body size between large- and small-bodied species, which is also associated with dental morphology, in that only small-bodied *Anoura* possess an enlarged paracone and reduced paracrista in the first upper premolar, and lack both the median internal cusp in the last upper premolar and the anteroexternal cuspid and cristid of the first lower molar (Allen, 1898; Mantilla-Meluk and Baker, 2006, 2010; Pacheco et al., 2018). Previous taxonomic schemes reflect these patterns of trait divergence. For example, based on differences in body size and dental characters, genus *Lonchoglossa* Peters, 1868 was used by Sanborn (1933, 1943), and later Husson (1962), to refer to individuals belonging to the small-bodied species *A. caudifer*. Other authors advocated for the use of a single genus name, *Anoura* (Simpson, 1945; Cabrera, 1958), and the generic name *Lonchoglossa* was eventually synonymized with *Anoura* (Tamsitt and Valdivieso, 1966). More recently, Mantilla-Meluk and Baker (2006, 2010) referred to small-bodied *Anoura* species as the "*A. caudifer* species complex" (including *A. aequatoris, A. cadenai, A. caudifer, A. fistulata*, and *A. luismanueli*) and to the large-bodied species as the "*A. geoffroyi* complex" (including *A. geoffroyi,* "*A. carishina,*" and *A. peruana*).

Over the past 15 years, *Anoura* taxonomy has been revisited extensively and remained in a state of flux (e.g. Muchhala et al., 2005; Simmons, 2005; Mantilla-Meluk and Baker, 2006, 2010; Griffiths and Gardner, 2008; Jarrín-V. and Kunz, 2008; Mantilla-Meluk et al., 2009; Pacheco et al., 2018; Díaz et al., 2016; Calderón-Acevedo, 2019; Cirranello and Simmons, 2020; Calderón-Acevedo et al., 2021). Díaz et al. (2016) recognized 10 *Anoura* species, and Pacheco et al. (2018) increased this number to 11 with the description of *A. javieri*. Nevertheless, there exists no single, widely agreed upon taxonomic classification for the genus, and the validity of several species remains debated. Mantilla-Meluk and Baker (2006) considered *A. aequatoris* to be a distinct species from *A. caudifer* based on discriminant analyses; however, others challenged their approach and conclusions, arguing that *A. aequatoris* should remain a subspecies (*A. c. aequatoris*) because its putatively diagnostic characters were unreliable (Jarrín-V. and Kunz, 2008, Griffiths and Gardner, 2008). This suggests that morphological variation attributed to *A. aequatoris* reflects polytypy within the broad geographical range of *A. caudifer* (Tamsitt and Valdivieso, 1966; Calderón-Acevedo and Muchhala, 2018). Similarly, Mantilla-Meluk and Baker (2010) suggested that *A. peruana* (Tschudi, 1844) should be considered distinct from *A. geoffroyi*, and they also described a new species, "*A. carishina*." Yet, recent morphological and molecular analyses failed to separate *A. peruana* from *A. geoffroyi* or "*A. carishina*" from *A. latidens* and strongly supported recognizing "*A. carishina*" as a junior synonym of *A. latidens* (Calderón-Acevedo, 2019; Calderón-Acevedo et al., 2021). Following recommendations of Griffiths and Gardner (2008), Jarrín-V. and Kunz (2008), Calderón-Acevedo (2019), and Calderón-Acevedo et al. (2021), *A. aequatoris*, "*A. carishina,*" and *A. peruana* should be considered synonymized, or non-distinct and in the process of synonymization. Thus, available evidence only unequivocally supports the following 8 *Anoura* species as valid and distinct: (1) *A. cadenai*, (2) *A. caudifer*, (3) *A. cultrata*, (4) *A. fistulata*, (5) *A. geoffroyi*, (6) *A. javieri*, (7) *A. latidens*, and (8) *A. luismanueli*.

To date, phylogenetic studies of *Anoura* have used limited taxon sampling, including only 3 or 4 of the species *A. caudifer, A. cultrata, A. geoffroyi* and *A. latidens* (Carstens et al., 2002; Datzmann et al., 2010; Rojas et al., 2012, 2016; Calderón-Acevedo et al., 2021; Fig. 1), and primarily focused on higher-level relationships, such as the position of *Anoura* within the subfamily Glossophaginae (Griffiths, 1982; Baker et al., 1989, 2003; Wetterer et al., 2000). Only three infrageneric phylogenetic hypotheses currently exist for *Anoura* (Fig. 1), including two hypotheses based on morphological and molecular data (Carstens et al., 2002; Dávalos et al., 2014), and a third hypothesis based solely on molecular data (Rojas et al., 2016). The time-calibrated phylogeny presented by Rojas et al. (2016) dated the common ancestor of four *Anoura* species to ~ 7.62 million years ago (Ma) in the Miocene. A recent study by Calderón-Acevedo et al. (2021) based on a subset of the genome-wide dataset analyzed herein recovered the same relationships as Dávalos et al. (2014; Fig. 1). However, the phylogenetic relationships of recognized *Anoura* species and species complexes remain largely unclear. Moreover, previous studies included only one small-bodied *Anoura* species, *A. caudifer*; thus, the monophyly of small-bodied and large-bodied *Anoura* has not been adequately tested.

Anoura present the widest geographical distribution of any genus within Glossophaginae, with species occurring from western Mexico through Central America, across South America from Colombia to Bolivia, and in Trinidad (Griffiths and Gardner, 2008). This wide geographical range is likely explained in part by high metabolic rates enabling *Anoura* to maintain more constant core body temperatures, and thus to inhabit higher elevations (Soriano et al., 2002). The Colombian Andes, with its three cordilleras, represents the geographical center of *Anoura* diversity, and seven known species have been recorded in Colombia (Fig. 2; Muchhala, 2006; Mantilla-Meluk and Baker, 2006; Griffiths and Gardner, 2008). Whereas *Anoura* species with smaller geographical ranges exhibit allopatric distributions consistent with vicariance and allopatric speciation, most *Anoura* species ranges are broadly sympatric with the two widest-ranging members of the genus. These species, *A. caudifer* and *A. geoffroyi*, inhabit many highland areas, the Brazilian Atlantic Forest, and the edges of lowland Amazonia, essentially encircling the Amazon Basin (Fig. 2; Mantilla-Meluk and Baker, 2006; Griffiths and Gardner, 2008). A time-calibrated phylogeny for *Anoura* based on improved taxon sampling is needed to allow inference of a broad-scale historical biogeographical scenario for the genus, in terms of where it originated and the main drivers of its tempo and mode of diversification.

In this study, we analyze a dataset of ultraconserved elements (UCEs) to conduct a phylogenomic study of *Anoura* species based on the most extensive taxonomic and genetic sampling of the genus to date. Ultraconserved elements have proven useful for resolving evolutionary relationships at different depths of divergence in tetrapods, including mammalian relationships (e.g. McCormack et al., 2012; Giarla and Esselstyn, 2015; Esselstyn et al., 2017; Morales et al., 2017; Van Dam et al., 2017; Andermann et al., 2019). Ours is the second study of *Anoura* based on genome-wide markers (after Calderón-Acevedo et al., 2021) and the first to infer *Anoura* relationships based on near complete species-level sampling (7/8 recognized species outlined above). It is also the first phylogenomic study of a genus within Phyllostomidae or Glossophaginae. We infer species trees using robust summary-statistic and quartet-based methods that have been shown to be statistically consistent under the multispecies coalescent (MSC; Chifman and Kubatko, 2014; Mirarab et al., 2014; Zhang et al., 2018), and we assess the potential impact of taxon sampling across loci on our phylogenetic inferences through a sensitivity analysis. We use our results to test previous hypotheses of *Anoura* relationships (Fig. 1) and taxonomy, and to test the monophyly of *Anoura* as well as its two species complexes. In addition to improving the resolution of interrelationships compared to previous studies based on fewer loci, we elucidate a historical biogeographical scenario for the genus using new chronograms of *Anoura* diversification. Our results contribute to a growing literature on Andean biogeography and systematics, ultimately providing a better understanding of mechanisms behind broad-scale patterns of diversification in

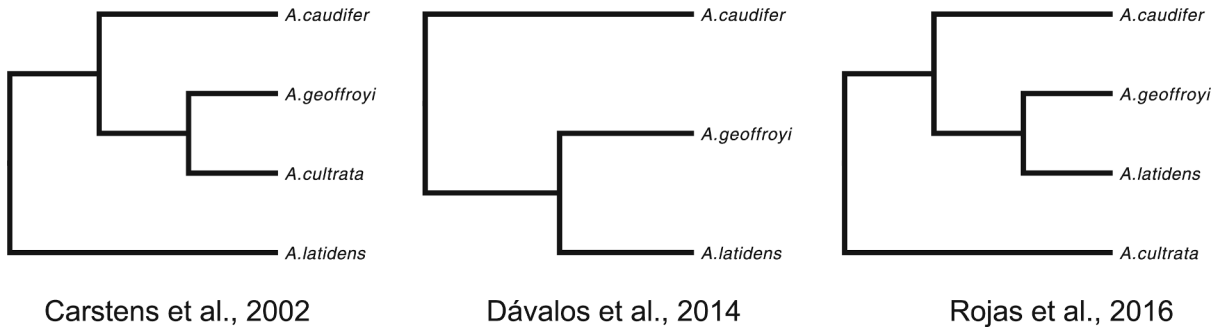

Fig. 1. Phylogenetic hypotheses of *Anoura* interrelationships based on previous morphological and molecular analyses. Cladograms were redrawn from studies listed in the figure.

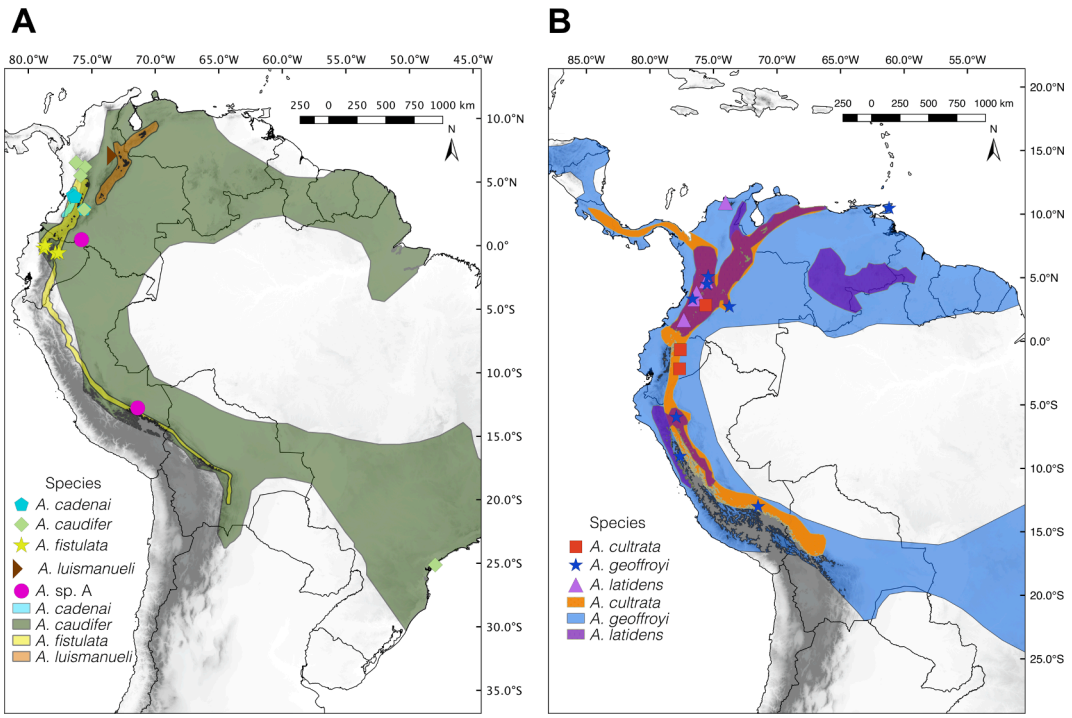

Fig. 2. Maps of sampling localities relative to the geographical distributions of *Anoura* species. Markers indicate sampling localities from this study, superimposed over range polygons for each species based on updated Noctilionoidea distributional data from Rojas et al. (2018). Separate maps are provided for (A) the "*A. caudifer* species complex" and (B) the "*A. geoffroyi* species complex" (Mantilla-Meluk and Baker, 2006, 2010), and the maps generally focus on higher-elevation regions of Central and South America with the highest concentrations of *Anoura* species, including the Tropical Andes.

the Northern Andes, which is one of the least studied yet most biotically diverse regions globally (e.g. Myers et al., 2000) and with regard to bat diversity (e.g. Rodríguez-Posada et al., 2021).

2. Materials and methods

2.1. Taxon sampling

We obtained tissue samples from 42 individuals representing 7/8 currently recognized species of *Anoura* (Fig. 2; Supplementary Tables S1, and S2) plus 1 candidate species (8 species/lineages in total). Of the recognized species, we only lacked samples from *A. javieri*. The candidate species, hereafter '*Anoura* sp. A', included two *Anoura* specimens that were morphologically similar but could not be confidently assigned by us, or other taxonomic experts, to nominal *Anoura* species based on external anatomy or tooth characters. Sampling included part of the type series of *A. cadenai* ($n = 3$), as well as specimens from the type series of the three taxa mentioned in Section 1 as being synonymized or non-distinct and in the process of synonymization (for details see Sections 3 and 4, Supplementary Tables S1 and S2). We also sampled two *Glossophaga* species for use as outgroups (*G. soricina*, $n = 1$; *G. longirostris*, $n = 1$). Samples from museum voucher specimens included in our study came from the following collections: Colección Teriológica Universidad de Antioquia (CTUA, Medellín, Colombia), Colección de Mamíferos Alberto Cadena García (ICN, Instituto de Ciencias Naturales, Universidad Nacional, Bogotá Colombia), Colección de Mamíferos Museo de Ciencias Naturales de la Salle (CSJ-m Instituto Tecnológico Metropolitano, Medellín, Colombia), Field Museum of Natural History (FMNH, Chicago, USA) and the Abilene Christian University Natural History Collection (ACUNHC, Abilene, TX, USA). Sampling is discussed further in Appendix A, and Supplementary Tables S1 and S2 list the voucher catalog numbers, geographical sampling localities, as well as NCBI BioProject and BioSamples accession numbers for all samples.

2.2. DNA extraction, UCE sequencing, and data processing

We extracted whole genomic DNA from ethanol-preserved tissues and museum skins using Puregene DNA Isolation Kits (Gentra System, Minneapolis, MN). Tissue samples from museum skins were prepared for extraction using a series of daily ethanol washes. Samples were immersed and vortexed in 99% ethanol with a subsequent 70% ethanol wash for 4 days to remove contaminants (Velazco and Patterson, 2013). RAPiD Genomics LLC (Gainesville, FL) was then tasked with sample library preparation and target enrichment of over 2386 UCEs in the tetrapod 2.5 K probe set (Faircloth et al., 2012), followed by multiplexed paired-end (PE) sequencing (2 × 100 bp) of UCEs on an Illumina HiSeq 3000 PE100 platform. We demultiplexed and assembled the resulting reads using the software program phyluce v1.6 (Faircloth, 2016, 2017). Demultiplexed reads were cleaned to remove low quality bases and adapter sequences in Trimmomatic (Lohse et al., 2012; Del Fabbro et al., 2013), as automated by the program Illumiprocessor (Faircloth, 2013). Subsequently, we performed *de novo* read assembly to obtain larger contigs using ABySS v1.5.2 (Simpson et al., 2009) with the default *k*-mer size value of 35. After probes and UCEs were matched, we aligned UCE contigs with MAFFT v7 (Katoh and Standley, 2013) using the default settings (–auto flag). We phased the final aligned contigs using the program 'phyluce_snp_bwa_multiple_align' available in phyluce, and then we extracted biallelic single nucleotide polymorphism (SNP) data from the BAM files using the phyluce program 'phyluce_snp_phase_uces'. Finally, phased SNPs were realigned across samples for each UCE locus using MAFFT v7 (Katoh and Standley, 2013).

The final dataset contained 2039 phased UCE loci with varying degrees of missing data for each of the 42 individuals and up to $n = 84$ phased sequences per locus (Table S2). To facilitate a sensitivity analysis evaluating the effects of taxon sampling on our phylogenomic species tree results, we split the concatenated alignment and filtered individual loci based on four different levels of taxonomic completeness, as follows (name, followed by taxonomic threshold percentage and number of loci in parentheses): 70p (70%, 1839 loci), 80p (80%, 1432 loci), 90p (90%, 432 loci), and 95p (95%, 100 loci). Loci in each filtered dataset met the sampling value threshold (%), while loci not meeting this threshold were excluded. Thus, increasing the threshold percentage also creates datasets with decreasing amounts of missing data. Prior to further analyses, sequence matrices for the full dataset (concatenated matrix with all loci) and each filtered dataset above were reduced to a single haplotype (allele) per gene per individual (selected at random, within each gene) using the 'dropRandomHap' function of PIrANHA v0.3a2 (Bagley, 2019). We combined all of the final 2039 UCE loci, filtered to one allele per individual per gene, into a concatenated 'supermatrix' (hereafter, 'concatenated dataset'). Raw Illumina reads generated during this study are available under NCBI BioProject PRJNA529738 (<http://www.ncbi.nlm.nih.gov/bioproject/529738 >). All Supplementary Material files, including aligned sequences, trees, and input files are available from a Mendeley Data accession for this project (available at: <http://dx.doi.org/10.17632/xhxbf5hyyt.1 >).

2.3. Phylogenomic analyses

2.3.1. Data partitioning

We inferred an optimum partitioning scheme for the final concatenated dataset, including the optimum number of data subsets (or 'partitions') and their DNA substitution models, in PartitionFinder v2.1.1 (Lanfear et al., 2014; Lanfear et al., 2017). Analyses used the relaxed hierarchical clustering algorithm ('rcluster' method), and the best scheme was selected based on the Bayesian information criterion (BIC). Due to computational demands, it was not possible to run the 'greedy' algorithm on our dataset (runs remained incomplete after 1 month of analysis on a supercomputing cluster). Also due to computational demands, and following other recently published empirical phylogenomics studies (e.g. Bagley et al., 2020), only the GTR + Γ model was used for phylogenetic analyses of our individual gene alignments below.

2.3.2. Gene tree analyses

We conducted multiple complementary gene tree analyses to infer the phylogeny of our focal taxa under concatenation methods, and also to provide gene trees for summary statistic-based species tree analyses below. First, we used the final concatenated dataset to infer the 'best' maximum-likelihood (ML) tree using concatenation + ML approach (CAML) in RAxML v8.2.12 (Stamatakis, 2014; -f a -x options, with 250 rapid bootstrapping iterations) while partitioning the data into partitions selected by PartitionFinder. Second, we used RAxML to infer gene trees for every UCE locus, specifying the GTR + Γ model and gauging nodal support based on 100 bootstrap pseudoreplicates, using the MAGNET v1.1.0 pipeline available in PIrANHA (Bagley, 2019). Gene trees were estimated for each gene in every filtered dataset (70p, 80p, 90p, 95p, and full datasets) as well. Third, we used SVDquartets v1.0 (Chifman and Kubatko, 2014, 2015) to estimate a multispecies coalescent gene tree, or 'lineage tree', for our full dataset based on quartet assembly methods. The lineage tree approach implemented in SVDquartets differs from the species tree approach in that a coalescent model is used but species labels are ignored and, instead of lumping tips into species assignments, each tip individual is treated as distinct. In SVDquartets, we set speciesTree=no and exhaustively sampled quartets and estimated node support using 500 non-parametric bootstrapping pseudoreplicates.

2.4. Species tree analyses

We inferred a species tree using two different approaches: (1) ASTRAL-III v5.6.3 (Mirarab et al., 2014; Zhang et al., 2018) and (2) SVDquartets. In our ASTRAL-III analyses, gene trees and bootstrap trees were used to estimate the species tree from every dataset (70p, 80p, 90p, 95p, and full datasets). ASTRAL-III computes a species tree from gene trees and provides internal branch lengths in coalescent units of gene tree discordance, as well as branch support values in the form of local posterior probabilities (LPPs) and multi-locus bootstraps. We ran multi-locus bootstrapping but decided not to include these values because LPPs are thought to have greater accuracy (*cf.* Sayyari and Mirarab, 2016). In our SVDquartets species tree analyses, we used a similar approach to that described in the previous section, except that in this case we repeated analyses twice, conducting independent species tree runs of SVDquartets on the full dataset while partitioning the data into either (1) all 2039 UCE loci or (2) the optimum data subsets identified by PartitionFinder. In each SVDquartets species tree run (with speciesTree=yes), quartets were exhaustively sampled and nodal support was estimated using 500 non-parametric bootstrapping pseudoreplicates.

2.5. Phylogenetic network reconstruction

Failing to consider the potential influence of introgressive hybridization among species can negatively impact phylogenetic inference (e.g. Solís-Lemus and Ané, 2016; Solís-Lemus et al., 2016; Olave and Meyer, 2020). Given the presence of unsupported nodes in our species tree and para-/polyphyletic species samples in our SVDquartets lineage tree (see Results), we evaluated the potential for reticulate evolution in our species tree using PhyloNetworks (Solís-Lemus et al., 2017), as implemented in Julia v1.4.1. Inference of phylogenetic networks was performed using maximum pseudolikelihood estimation in SNaQ (Solís-Lemus and Ané, 2016). To potentially reduce gene tree error and improve our PhyloNetworks analyses, we re-estimated gene trees for each locus after (1) trimming sequences and (2) pruning alignments down to one individual per species. Sequence trimming was conducted in trimAl (Capella-Gutiérrez et al., 2009), as automated in the 'trimSeqs' function of PIrANHA v0.4a3 (Bagley, 2020); here, sequences were trimmed using a trimAl conservation threshold of 60%, and then UCE

loci with greater than 98% sequence identity were filtered out. We pruned *Glossophaga* outgroups from the alignments for the remaining loci in R using the 'drop.tip' function of the APE package (Paradis and Schliep, 2015). Gene tree estimation was conducted on the trimmed and pruned alignments in RAxML using procedures identical to those above (Section 2.3.2). Additionally, in an attempt to reduce spurious inferences of gene flow (reticulation events) caused by variable taxon sampling (Solís-Lemus et al., 2017), we supplied SNaQ with unrooted gene trees from 899 UCE loci containing at least one individual representative for each of our 8 ingroup focal species/lineages. Observed concordance factors (CFs) were calculated from the final 899 gene trees and used to infer semi-directed phylogenetic networks with different maximum numbers of reticulation events ($h = [0, 1, 2]$; using 20 independent runs per h-value) and the proportion (γ) of genomic ancestry in the hybrid lineage contributed by each parental species/lineage. Support for an appropriate h value for our dataset was assessed using the graphical slope heuristic, with pseudolikelihood score plotted against h ('hmax'), as described by Solís-Lemus et al. (2017). We also compared the fit to our data of a coalescent model explaining gene tree discordance due to incomplete lineage sorting (ILS), versus the $h = 1$ network, by extracting and graphically plotting the fit based on expected versus observed CFs, as explained in the SNaQ/PhyloNetworks documentation.

2.6. Divergence time and demographic parameter estimation

We inferred divergence times and demographic parameters for *Anoura* species and lineages using two methods: (1) gene tree calibration using penalized likelihood (PL; Sanderson, 2002) in treePL (Smith and O'Meara, 2012), and (2) parameter estimation over the species tree in a Bayesian coalescent framework in BPP v4.3.0 (Rannala and Yang, 2003; Yang, 2015; Flouri et al., 2018). For the penalized likelihood method, we obtained divergence times in treePL by calibrating the best ML tree from the analysis of the full concatenated dataset (see Section 2.2), and using two secondary calibration points based on divergence dates inferred by Rojas et al. (2016) in a multilocus phylogenetic analysis of Noctilionoidea. Calibration points included the upper and lower 95% credible intervals of the most recent common ancestor (MRCA) date estimates for the divergence of *Anoura* and *Glossophaga* (22.21–17.22 Ma) and of all *Anoura* species (9.75–5.03 Ma). We ran treePL multiple times with random seeds, using the 'thorough' run mode and the 'leave one out' cross-validation procedure.

For the Bayesian method, we estimated the divergence times (τs) and population size parameters ($\theta = 4N_e\mu$, where N_e is the effective population size and μ is the substitution rate per site per generation) of *Anoura* species and lineages using 'A00′ parameter estimation analyses in BPP (speciesdelimitation = 0 and speciestree = 0 settings). Given that a phylogenetic network allowing reticulations did not improve model fit based on heuristics (see Results), we ran BPP under the standard MSC model implemented in BPP (Rannala and Yang, 2003) and not the MSC-with-introgression model (MSci; Yu et al., 2014; Flouri et al., 2020). Analyses were run while fixing the species tree to the topology estimated in ASTRAL-III (which was identical to that inferred in SVDquartets; see Results), and were conducted in six independent runs (three with, versus three without removing sites with ambiguity data using cleandata = 1) to confirm consistency of results. We set the inverse-gamma priors to $\theta \sim$ IG(3, 0.002) for θ parameters and to $\tau_0 \sim$ IG(3, 0.004) for the root τ parameter, and we used a Dirichlet distribution (a = 3) for all other τs (*cf.* Flouri et al., 2020). Each run consisted of 250,000 MCMC iterations (sampled every other iteration; sampfreq = 2) following a burn-in period of 50,000 iterations, and used custom finetune settings based on pilot runs. Convergence and MCMC chain mixing were assessed in R using graphical plots and summaries of parsed log files, in part using the tracerer package (Bilderbeek and Etienne, 2018). Posterior estimates from BPP were converted to absolute time in the bppr (Angelis and dos Reis, 2015; dos Reis, 2020) R package using the *Anoura* MRCA calibration from Rojas et al. (2016) mentioned above, while assuming a generation time of one year (Galindo-Galindo et al., 2000).

2.7. Historical biogeography

We reconstructed the geographical distributions and dispersal events of *Anoura* using the BioGeoBEARS R package (Matzke, 2013a, 2016) and the final time-calibrated species tree from BPP, with one tip per species/lineage. We used area-codings based on dividing the geographical ranges of *Anoura* species/lineages into the following regions: the Brazilian Atlantic Forest, or 'Mata Atlântica' (M); Amazonia (A); the Central Andes (C) of Peru and Ecuador; the Northern Andes (N) of Colombia; and the Lesser Antilles (T). We tested three models, including Dispersal-Extinction-Cladogenesis (DEC; Ree and Smith, 2008), a likelihood version of the parsimony Dispersal-Vicariance model (DiVA; Ronquist, 1997) called 'DIVALIKE', a likelihood version of the BayArea model (Landis et al., 2013) called 'BAYAREALIKE'. The maximum likelihood framework implemented in BioGeoBEARS for the DIVALIKE and BAYAREALIKE models allows direct comparison of model fit using standard information-theoretic approaches to model selection. We used the Akaike Information Criterion (AIC; Akaike, 1974) and the AIC corrected for small sample size (AICc) to statistically compare the fit of the models to our data under AIC model selection (Burnham and Anderson, 2002, 2004).

The DEC model (Ree and Smith, 2008) assumes that daughter lineages inherit the ancestral area state if the MRCA is limited to a single area, while if the MRCA has a widespread distribution then one of the daughter lineages will inhabit only a smaller single area within the ancestral area. On the other hand, DiVA (Ronquist, 1997) reconstructs ancestral distributions without assumptions about the relationships between areas and assumes that speciation depends on vicariance events. Finally, the BayArea model assumes that there is no range evolution at cladogenesis and thus the ancestral range is inherited by both daughter species. This model also allows for the inclusion of a large number of areas (Landis et al., 2013; Matzke, 2013b).

3. Results

3.1. DNA extraction, UCE sequencing, and data processing

We obtained a total of 179,809,722 raw PE reads, with an average of 4,281,184 reads per individual (range: 765,774–7,704,220), 499,242 contigs per individual (range: 88,262–857,926), and 1891 UCE loci per individual (range: 1423–1965). The matrix of sequences for the 2039 UCE loci in the full concatenated dataset contained 986,712 aligned nucleotides, with slightly elevated A and T frequencies but lower GC content (A: 29.6%; C: 20.5%; G: 20.5%; T: 29.4%). Overall, this dataset was highly informative, with 51,103 variant sites or SNPs, of which 38,047 were parsimony-informative sites (range: 0–129 parsimony-informative sites per UCE locus).

3.2. Phylogenomic analyses

Our CAML analysis of the full concatenated dataset yielded a well-resolved gene tree topology with four major clades (clades 1–4), with definitive support (BP = 100) for all clade-level nodes and other internal nodes (Fig. 3A). However, tip nodes had lower support, leading to lower nodal support overall (mean BP = 73.6). The lineage tree from our SVDquartets analysis of the full concatenated dataset under the MSC was also well resolved (Fig. 3B), with high bootstrap support for internal nodes, and was largely congruent with the CAML gene tree. The lower, more variable support for mid-crown to tip nodes was expected, given that many of these nodes subtended individuals of the same species. Both trees contained the following relationships. Clade 1 included the small-bodied species, *A. cadenai* and *A. fistulata*, and placed the candidate species *A.* sp. A as sister to *A. cadenai*. Clade 2 contained the other small-bodied *Anoura* species, *A. caudifer*, with the single *A. luismanueli*

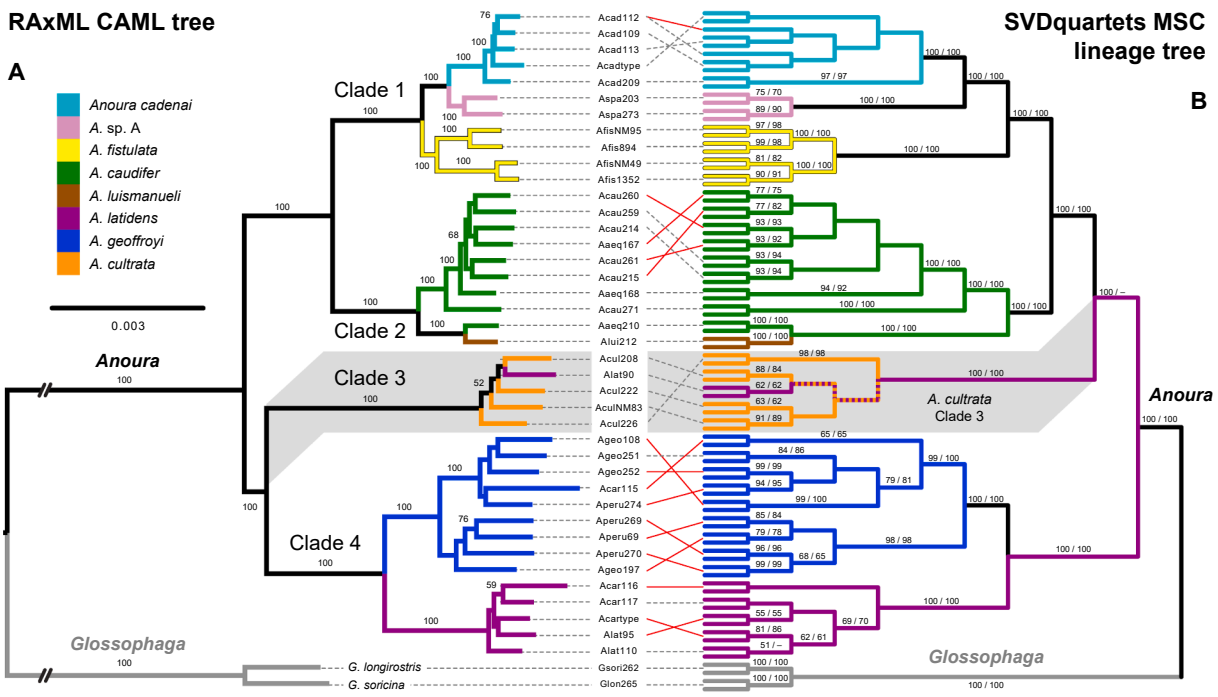

Fig. 3. Tanglegram comparisons of the best gene tree from concatenation + ML (CAML) analysis in RAxML (A; Stamatakis, 2014) and the multispecies coalescent (MSC) lineage tree from SVDquartets (B; Chifman and Kubatko, 2014) inferred from 2039 UCEs in the full dataset including 40 *Anoura* individuals and two *Glossophaga* outgroups. RAxML results include bootstrap proportion (BP; %) support values along nodes and scale bar in units of substitutions/site. SVDquartets results have nodal support values expressed in the following format: bootstrap proportion (%) from analysis partitioning the data into optimal subsets derived from PartitionFinder 2 / bootstrap proportion (%) from analysis partitioning the data by UCE locus. Branches are colored in accordance with four major clades we identified and red tanglegram lines indicate incongruent tip taxon placements or groupings. Shaded boxes enclose subclades discussed in the text. (For interpretation of the references to color in this figure legend, the reader is referred to the web version of this article.)

sample nested among the *A. caudifer* samples. Clade 3 was comprised of *A. cultrata* samples, within which a single sample of *A. latidens* (Alat90) was interdigitated. Last, clade 4 consisted of samples of the large-bodied species *A. geoffroyi* + *A. latidens* in a sister relationship. Aside from minor tip differences within species/lineages (see tanglegram lines), the main point of incongruence between gene trees involved the placement of the *A. cultrata* clade (clade 3); the RAxML CAML tree inferred this clade as sister to the predominantly large-bodied *Anoura* clade 4, while the SVDquartets lineage tree inferred it to be sister to the predominantly small-bodied clade comprised of clades 1 and 2.

Several additional patterns of congruence among our gene trees also warrant highlighting due to their taxonomic implications. First, both trees placed the small-bodied species *A. fistulata*, *A. caudifer*, and *A. cadenai* together in a clade (clades 1 + 2) including *A.* sp. A, which we consider the *A. caudifer* species complex (*cf.* Mantilla-Meluk and Baker, 2006). Second, both trees placed the large-bodied species *A. geoffroyi* and *A. latidens* together in a separate clade (clade 4), which we consider the *A. geoffroyi* complex (*cf.* Mantilla-Meluk and Baker, 2010). Third, samples formerly attributed to "*A. carishina*" (including the type specimen, Acartype) were nested within *A. latidens*, consistent with a recent study synonymizing the former within the latter species (Calderón-Acevedo et al., 2021). Fourth, samples of *A. caudifer* formed a single lineage, which was largely cohesive despite the very wide geographical distribution of this species, with one sample from the Brazilian Atlantic Forest (Acau271) being strongly supported as sister to a large clade of samples from the Andes Mountains. Samples corresponding to the dubious taxon *A. aequatoris* ("Aaeq" sample ID prefixes; sometimes referred to as subspecies *A. c. aequatoris*; Jarrín-V. and Kunz, 2008) were polyphyletic and did not form a distinct species or monophyletic sub-lineage. Our only sample of *A. luismanueli* also grouped within the *A. caudifer* clade. Last, samples identified as *A. geoffroyi* formed a cohesive group, but samples corresponding to the dubious taxon *A. peruana* ("Aperu" sample ID prefixes; sometimes referred to as subspecies *A. geoffroyi peruana*) were polyphyletic, indicating that they do not form a distinct species or a monophyletic sub-lineage, but rather should be referred to as *A. geoffroyi*.

Several important biogeographical patterns were also apparent among our gene tree results. In particular, *A. fistulata* samples from the western slopes of the Andes (Afis894 and AfisNM49) formed a strongly-supported clade sister to those from the eastern slopes (AfisNM95 and Afis1352), indicating an allopatric divergence. Additionally, one sample of *A. caudifer,* Aaeq210 (previously attributed to *A. aequatoris*), was sister to the only sample of *A. luismanueli* (Alui212) included in our study. Finally, one individual from the Northern Andes that is morphologically diagnosable as *A. latidens* (Alat90; ICN-4398) was phylogenetically nested within our *A. cultrata* samples. Both trees infer this individual, Alat90, to be sister to a lineage containing a specimen of *A. cultrata* (Acul208; ICN-21196) from the western slope of the Andean Cordillera Central.

3.3. Species tree analyses

The ASTRAL-III species tree estimated from the full UCE dataset contained four main clades (Fig. 4A) that were identical to relationships in our RAxML CAML tree (Fig. 3A). Local posterior probability support values were 1.0 for all splits in the ASTRAL-III species tree with the exception of the node representing the sister relationship between clades 3 and 4, which was also highly supported by a local posterior probability value of 0.98. ASTRAL-III species trees computed from the reduced 70p, 80p, and 90p datasets, with taxon completeness at 70%, 80%, and 90%, respectively, had topologies similar to that of the full dataset, suggesting that varying taxon sampling and missing data levels had minimal impact on our species tree inferences (see Supplementary Fig. S1). However, the ASTRAL-III species tree derived from the 95p dataset reconstructed

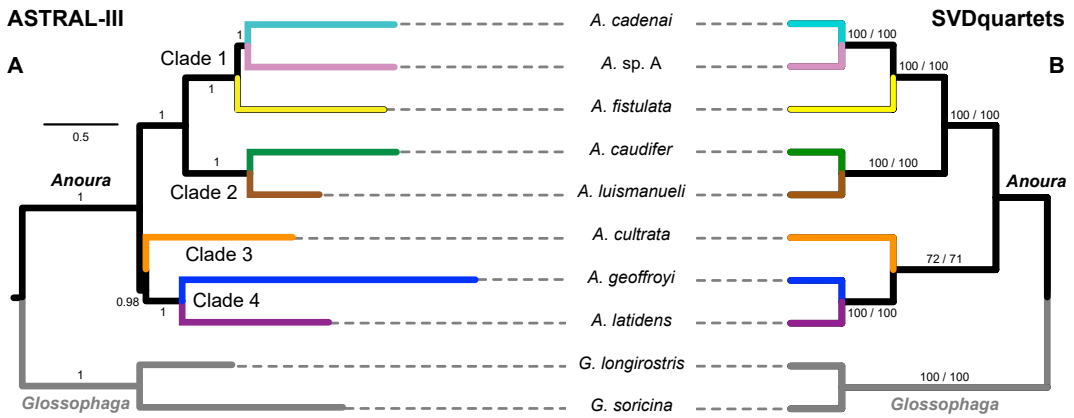

Fig. 4. Tanglegram comparisons of species tree relationships among *Anoura* species/lineages reconstructed using gene tree summarization in ASTRAL-III (A; Mirarab et al., 2014; Zhang et al., 2018) versus the phylogenetic invariants-based method implemented in SVDquartets (B; Chifman and Kubatko, 2014). Results are shown from analyses of gene trees derived for each UCE locus in ASTRAL-III, and from an analysis of the 2039 UCEs in the full dataset in SVDquartets under the multispecies coalescent model while mapping individuals to species to generate a species tree. The ASTRAL-III species tree is labeled with local posterior probabilities (Sayyari and Mirarab, 2016) and a scale bar is provided in coalescent units. SVDquartets nodal support values and other formatting follows details described in the caption to Fig. 3.

A. cultrata as sister to the *A. caudifer* species complex rather than to clade 4, albeit with very low posterior support (0.41; Supplementary Fig. S1).

The species tree inferred from the full dataset in SVDquartets was topologically identical to our ASTRAL-III species tree, thus tanglegram lines did not overlap (Fig. 4B). Inferred relationships were all strongly supported with 100% bootstrap support in this tree, with two exceptions. First, the node grouping *A. cultrata* in clade 3 with the larger-bodied species *A. geoffroyi* and *A. latidens* in clade 4 had bootstrap support ranging from 71% to 72% (Fig. 4B). Second, whereas *Anoura* was strongly supported as monophyletic in the ASTRAL-III results, the crown node never received bootstrap support greater than 50% in the SVDquartets species tree.

3.4. Phylogenetic network reconstruction

Our PhyloNetworks analyses revealed that a model increasing the number of reticulations from $h = 0$ to $h = 1$ did not provide a substantially better fit to our data than a model with strictly bifurcating trees, in which gene tree discordance is explained by ILS alone. First, the heuristic inference from plotting the pseudolikelihood score (−loglik) against the maximum number of reticulation events (hmax) for each model revealed a very modest slope (Supplementary Fig. S2A), rather unlike the strong downward slopes obtained in studies where authors accepted the network as providing a superior fit to the data (Solís-Lemus et al., 2016, 2017; Blair et al., 2019). Second, graphical plot-based tests of goodness-of-fit showed that allowing a single reticulation in the $h = 1$ network did not improve the fit to our data over a coalescent model assuming $h = 0$. Specifically, the relationship between the expected versus observed gene tree discordance among quartets, summarized by CFs (using frequencies of 3 quartets in the gene trees) was not improved by allowing one reticulation, as points were no closer to the diagonal (1:1) line under $h = 1$ than under $h = 0$ (Fig. S2B; see the SNaQ/PhyloNetworks documentation for details). Subsequently, we only discuss results from our fully bifurcating gene trees and species trees.

3.5. Divergence times and demography of Anoura species

Chronograms from treePL (Fig. 5A) and BPP (Fig. 5B) analyses yielded divergence time estimates that were largely congruent and revealed that *Anoura* is a relatively recent Neogene genus. The time-calibrated treePL tree dated the most recent common ancestor (MRCA) of *Anoura* to ~ 6.67 Ma in the Miocene, which corresponds to the initial divergence between the large- and small-bodied *Anoura* clades (clades 1 + 2 vs. clades 3 + 4), with subsequent intra-lineage diversification events occurring largely over the Pliocene to Pleistocene (Quaternary; Fig. 5A). Evolutionary divergence of the three species in the large-bodied clade (clades 3 + 4) dated to ~ 6.33 Ma in the late Miocene, and diversification within the *A. geoffroyi* species complex was marked by an initial divergence at the MRCA ~ 4.05 Ma in the Pliocene, while population divergence within *A. cultrata* began around 1.68 Ma in the Pleistocene. We also infer that diversification within *A. geoffroyi* and *A. latidens* has occurred since around 2.8 Ma and 1.1 Ma, respectively. Within the small-bodied *A. caudifer* species complex, we infer that its two major lineages diverged around 4.7 Ma in the Pliocene. While the *A. caudifer* MRCA date indicates genetic variation has arisen since ~ 2.5 Ma at the Plio–Pleistocene boundary, all other species within this complex speciated or experienced intraspecific genetic divergences soundly within the Pleistocene epoch (MRCAs: *A. fistulata*, 2.13 Ma; *A.* sp. A, 1.20 Ma; *A. cadenai*, 0.81 Ma; *A. luismanueli*, 1.02 Ma; Fig. 5A).

Our BPP chronogram, from A00 analysis estimating parameters over the species tree, dated the *Anoura* MRCA to ~ 7.4 Ma in the Miocene, which was only ~ 0.8 Ma older than the treePL chronogram, with subsequent diversification largely over the Pliocene to Pleistocene (Quaternary; Fig. 5B). Within the large-bodied clade, the divergence of its three species dated to ~ 5.09 Ma in the Pliocene, and diversification within the *A. geoffroyi* species complex is marked by an initial divergence at ~ 4.85 Ma in the Pliocene. From the time-calibrated BPP tree, we infer a slightly older date for the initial divergence of the small-bodied *A. caudifer* species complex of 5.5 Ma, which is near the Miocene–Pliocene boundary. Within this complex, the BPP tree dated the *A. cadenai–A.* sp. A divergence at 2.25 Ma, the clade 1 (*A. cadenai–A.* sp. A–*A. fistulata*) MRCA at 3.24 Ma, and the *A. caudifer–A. luismanueli* divergence within clade 2 at 1.39 Ma (Fig. 5B), all within the Pleistocene. The N_e estimates for *Anoura* species/lineages from BPP are represented by branch widths in Fig. 5B and ranged from 35,776 individuals for the MRCA of clade 1 to 721,322 individuals for the *A. caudifer* tip lineage (Supplementary Table S3).

3.6. Historical biogeography

In our BioGeoBEARS analysis, we found that DEC model outperformed all other models (Table 1). The DEC model had the highest ln *L* score, but this model was statistically indistinguishable from the next best model based on ΔAIC < 2.0 (Burnham and Anderson, 2002, 2004). For simplicity of interpretation and presentation of results, we conservatively accepted the model with the lowest AICc score and number of

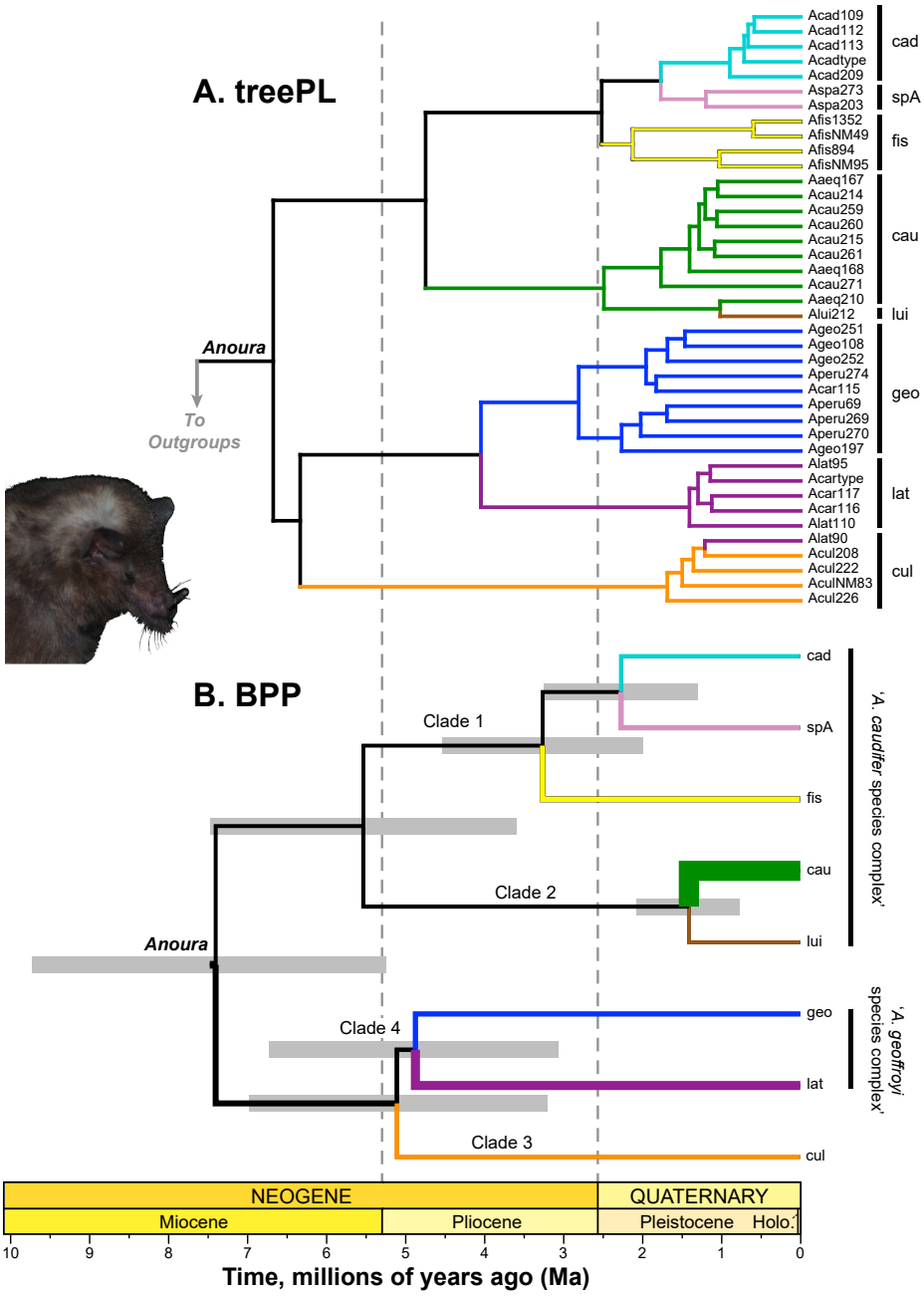

Fig. 5. Time-calibrated phylogenies for *Anoura* based on penalized likelihood analysis of the concatenation tree from RAxML in treePL (A; Smith and O'Meara, 2012) and estimation of divergence times and population sizes over the species tree in BPP (B; Rannala and Yang, 2003; Yang, 2015; Flouri et al., 2018). Results are presented with the *y*-axis in units of time in millions of years ago (Ma), with branches colored to match clades as in Figs. 3 and 4. In panel (B), branch widths are scaled proportional to effective population size (N_e) converted from BPP θ parameters, with the thinnest branch corresponding to $N_e \approx 36{,}000$ and the thickest branch corresponding to $N_e \approx 721{,}000$ (details in Supplementary Table S3). The full treePL time tree, including outgroup taxa, is provided in Fig. S3.

parameters (K) as the best-supported model. Hereafter, ancestral area reconstructions and other BioGeoBEARS results are only discussed for the DEC analysis of the BPP species tree.

The ancestral range of the MRCA of *Anoura* was reconstructed as occupying all five geographical regions in our area-coding scheme (Fig. 6). The MRCA of both main clades, the large-bodied clade containing *A. cultrata* + the *A. geoffroyi* species complex, and the *A. caudifer* species complex was reconstructed in four areas, including all regions except for the Lesser Antilles. These results suggest that multiple *Anoura* lineages likely had overlapping geographical ranges since their initial divergence, over Miocene–Pliocene, but there is high uncertainty in the earlier ancestral range estimates at deeper nodes of the phylogeny.

Anoura clade 1 (*A. cadenai*, *A.* sp. A, and *A. fistulata*) exhibited a pattern of fragmentation of an ancestral range spanning the Central and Northern Andes plus the Amazon Basin, with the *A. fistulata* MRCA remaining in the Northern Andes Mountains, while the MRCA of *A. cadenai* and *A.* sp. A evolved within all three areas (Fig. 6). Allopatric divergences were reconstructed between *A. cadenai* in the Northern Andes and *A.* sp. A in the Central Andes and Amazon Basin. In contrast to results for *Anoura* clade 1, the MRCA of *A. caudifer* in clade 2 as experiencing fragmentation of a wide range encompassing four areas while *A. luismanueli* was reconstructed as remaining in the Northern Andes. For the clade 3 *A. cultrata* lineage, the ancestor was reconstructed as inhabiting the Central and Northern Andes based on the species tree (Fig. 6). For clade 4, the *A. geoffroyi* species complex was reconstructed as having a wide geographical distribution across all five areas, with subsequent fragmentation of the MRCA of *A. latidens* and *A. geoffroyi*.

4. Discussion

4.1. Phylogenetic relationships among Anoura species

Recent studies, based on limited sampling in terms of taxa and genes, have reconstructed conflicting phylogenetic relationships among

Table 1
Comparison of models used to reconstruct the biogeographic history of *Anoura* species/lineages in BioGeoBEARS using the time-calibrated BPP species tree (n = 8 tips).

Model	ln L	Parameters	d	e	AIC	AICc
DEC	**−21.71**	**2**	**0.064**	**1.00×10^{-12}**	**47.4**	**49.8**
DIVALIKE	**−22.46**	**2**	**0.075**	**1.00×10^{-12}**	**48.9**	**51.3**
BAYAREALIKE	−24.99	2	0.054	0.12	54	56.4

Results are shown for AIC-based comparisons among three models run in BioGeoBEARS on the BPP species tree, converted to absolute time using the bppr R package. Models are discussed in further detail in the text (Section 2.7), and the geographical areas that were modeled are also shown in Fig. 6. Results from the 'best supported' model are shown in boldface; where models were indistinguishable (ΔAIC < 2.0), results show two models in boldface. Abbreviations: AIC, Akaike information criterion (Akaike, 1974); AICc, small sample size-corrected Akaike information criterion; d, rate of dispersal (range expansion); e, rate of extinction (range contraction; ln L, log-likelihood score of the model.

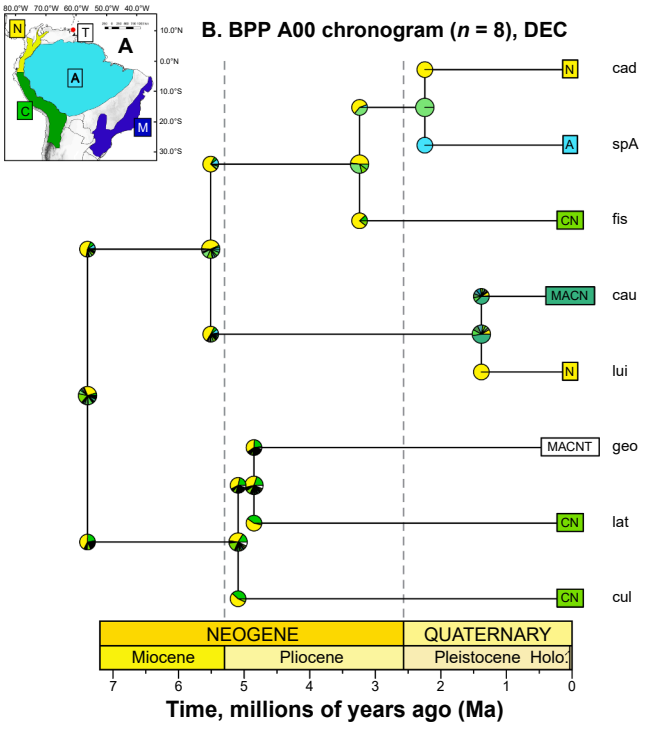

Fig. 6. Area codings (A) and ancestral ranges for 8 species/lineages of *Anoura* sampled in this study reconstructed in BioGeoBEARS using the DEC model over the BPP species tree (B). Pie charts at nodes illustrate the inferred ancestral areas, while those at branch corners illustrate areas of descendant lineages formed by instantaneous speciation events. Area codings for the known present-day distributions of each species/lineage (extending beyond our sampling, where applicable; see Fig. 2) are presented at the tips of each phylogeny. Results are presented only for the best-supported model inferred during model selection, as shown in Table 1 and discussed in Section 3.6 of the text.

Anoura leaf-nosed bats (Carstens et al., 2002; Dávalos et al., 2014; Rojas et al., 2016; Fig. 1). Here, we used a phylogenomic approach based on data from thousands of UCE loci to infer phylogenetic relationships, divergence times, and a historical biogeographical scenario for *Anoura* bats. UCEs are highly reliable for phylogenetic inference, given their verified homology, low saturation, and typically lower GC content reflecting reduced recombination rates (e.g. Faircloth et al., 2012; McCormack et al., 2012; Esselstyn et al., 2017). Additionally, our data represent the most loci (i.e. genetic sampling) evaluated for *Anoura*, by orders of magnitude, as well as the most extensive taxonomic coverage (~88%; 7/8 currently valid species) of the genus in phylogenetic studies to date. Our results based upon these data strongly supported the reciprocal monophyly of *Anoura*, consistent with previous studies (Carstens et al., 2002; Dávalos et al., 2014; Rojas et al., 2016; Fig. 1). Our study was also the first to strongly support the monophyly of the small-bodied *A. caudifer* species complex and the large-bodied *A. geoffroyi* complex recently recognized by Mantilla-Meluk and Baker (2006, 2010), based on 100% taxon-sampling of each complex. Additionally, all clade- and species-level relationships in our trees had high to definitive nodal support values (BP ≥ 70 and local posterior probability ≥ 0.98; Figs. 3, 4, and S1), and multiple concatenation- and coalescent-based analyses making different assumptions obtained largely congruent results supporting a preferred ingroup topology of the form, ((((*A. cadenai*, *A.* sp. A), *A. fistulata*),(*A. caudifer*, *A. luismanueli*)), (*A. cultrata*,(*A. geoffroyi*, *A. latidens*))).

Overall, the high bootstrap and local posterior probability support values inferred for our gene trees and species trees suggest that UCEs and multiple analytical approaches were able to confidently resolve relationships along the *Anoura* branch of the Tree of Life. Thus, we recommend UCE studies for resolving phylogenetic relationships within and among other genera in Phyllostomidae and Glossophaginae. Still, systematic errors remain a concern in analyses of large phylogenomic datasets. Issues arguably of the greatest relevance for UCEs include long-branch attraction (LBA; e.g. Felsenstein, 1978), missing data effects (taxon and locus levels; e.g. Hosner et al., 2016), and the possibility of inconsistency with inflated BPs supporting incorrect relationships in trees derived from concatenation analyses (e.g. Kumar et al., 2012; Roch and Steel, 2015). It is therefore common in phylogenomics studies to rely on topological congruence among methods, rather than individual BPs, when assessing confidence in results (e.g. Suh, 2016). We found results from different inference methods to be overall highly congruent, with limited exceptions. We also found no evidence among our results for LBA, which we believe was mitigated by our use of near-comprehensive taxon sampling to effectively break up longer branches. Additionally, our sensitivity analysis showed that ASTRAL-III results were relatively robust to variable taxon sampling across loci, which was correlated in our filtered datasets with total numbers of loci (Fig. S1). However, we obtained higher BPs in our CAML tree than the SVDquartets lineage tree (Fig. 3), which suggests that SVDquartets more adequately accounted for uncertainty due to ILS in our dataset (*cf.* Esselstyn et al., 2017). In a conspicuous exception to the overall high support values across our results, the *Anoura* crown node did not receive definitive nodal support in the SVDquartets species tree (Fig. 4B). To investigate this pattern further, we checked our results and found that *Glossophaga* outgroup specimens fell within the ingroup in approximately 12.6% individual gene trees (190/1510 rooted gene trees containing *G. longirostris*; unpublished results). We note that, based on phylogenetic results in Rojas et al. (2016), *Glossophaga* is a relatively distant outgroup, with at least five major lineages comprising 9 genera of phyllostomid bats separating it from *Anoura*. Thus, the low crown node support in our SVDquartets lineage tree most likely is due to homoplasy via convergent evolution (*cf.* Funk and Omland, 2003), which has resulted in the relatively distant outgroup sharing fewer character states with the ingroup than more proximal lineages. This interpretation seems likely to be correct even despite the slow substitution rates of UCEs (e.g. Faircloth et al., 2012; McCormack et al., 2012) because the distance between *Glossophaga* and *Anoura* has allowed a great deal of time—over 10 million years (Myr; Rojas et al., 2016)—for the accumulation of homoplasy. However, given congruence among our other results, particularly our species trees, we conclude that homoplasy has not unduly influenced our results overall.

Within the small-bodied *A. caudifer* species complex, we found that *A. fistulata* and *A. cadenai*, the two largest species in the complex (Calderón-Acevedo, 2019), formed a clade with a morphologically distinct and highly genetically distinct candidate species that we refer to

as *Anoura* sp. A. This new candidate species is strongly supported as sister to *A. cadenai* across our gene tree and species tree results, with definitive support (Figs. 3 and 4), and this novel insight allows us to broaden the definition of the *A. caudifer* species complex (sensu Mantilla-Meluk and Baker, 2006) to also include *A.* sp. A in addition to *A. caudifer*, *A. cadenai*, and *A. fistulata*. The four individuals of *A. fistulata* in our sample grouped together in our phylogenies but exhibited a deep genetic split across the eastern and western versants of the Central Andes Mountains of Ecuador, with this relationship and each subclade receiving high nodal support. Also in this complex, *A. caudifer* remained largely cohesive as a species, with a sample from Brazil inferred as sister to all Andean individuals (Fig. 3). *Anoura caudifer* is widely recognized as the most phenotypically variable species within the genus, as it exhibits variation in body size and skull shape throughout its range (Jarrín-V. and Kunz, 2008; Jarrín-V. and Coello, 2012; Calderón-Acevedo and Muchhala, 2018). Others hypothesized that this variation may reflect a latitudinal cline in size variation, and similar patterns of variation have previously been documented from higher to lower latitudes in *A. cultrata* (Nagorsen and Tamsitt, 1981; Tamsitt and Nagorsen, 1982).

Our phylogenetic results also showed that the *A. geoffroyi* species complex, including *A. geoffroyi* and *A. latidens* (Mantilla-Meluk and Baker, 2010), formed a cohesive clade (clade 4) that we inferred to be sister to *A. cultrata* (clade 3) with high nodal support in most analyses (Figs. 3, 4 and S1). Results from only one of our main analyses deviated from this relationship: the SVDquartets lineage tree instead inferred the *A. cultrata* clade to be sister to the small-bodied *A. caudifer* species complex in clades 1 + 2 (Fig. 3B). One common source of such incongruences among phylogenomic results is ILS, which often causes gene trees to be discordant with the true species tree. Because of this, we opted to use two coalescent-based species tree approaches, ASTRAL-III and SVDquartets, that have been shown to be consistent and to perform well at species tree estimation in the face of ILS (Chifman and Kubatko, 2014; Mirarab et al., 2014; Sayyari and Mirarab, 2016; Zhang et al., 2018). ASTRAL-III is also more robust to gene tree errors than other summarization methods (Mirarab and Warnow, 2015). Given that these species tree methods account for ILS and gene tree discordance in different ways, but converged on the same topology (Fig. 4), we take the species tree results placing *A. cultrata* as sister to *A. geoffroyi* and *A. latidens* as our preferred phylogenetic hypothesis.

Contrasting the broadly congruent and monophyletic relationships among our results, we inferred two paraphyletic patterns of valid *Anoura* species in our gene trees. First, our only *A. luismanueli* sample (Alui212) was nested within clade 2, rendering *A. caudifer* paraphyletic (Fig. 3). Although *A. luismanueli* is currently recognized as a valid species, it was only recently reported from Colombia (only the Cordillera Oriental; Mantilla-Meluk and Baker 2006) and thorough comparisons between Colombian and Venezuelan specimens are lacking. Additionally, *A. luismanueli* morphological measurements overlap with *A. cadenai*, *A. caudifer*, and *A. fistulata* (Jarrín-V. and Kunz, 2008; Calderón-Acevedo and Muchhala, 2018) and its diagnosis relies on geographic distribution and subjective unquantified characters such as amount of fur on the uropatagium. The above finding suggests that *A. luismanueli* may need to be subsumed within *A. caudifer*; however, additional sampling and geographic coverage are needed to evaluate this hypothesis more robustly. The second paraphyletic pattern involves sample Alat90, which we infer as nested within *A. cultrata* samples in clade 3. This specimen, which is from the Cordillera Oriental of Colombia, has all external anatomical characteristics diagnostic of *A. latidens* and also lacks the blade-like lower premolar (p1) character unique to *A. cultrata* (Handley, 1960, 1984; Calderón-Acevedo et al., 2021). By contrast, the sister lineage to Alat90 is a specimen of *A. cultrata* (Acul208) from the western slope of the Andean Cordillera Central that lacks the dental characteristics of *A. latidens* [i.e. possesses no triangular last upper premolar (P4) with base of the tooth enclosing the medial-internal cusp], and which possesses a blade-like first lower premolar. Thus we do not believe this reflects a simple case of misidentification. Furthermore, as we obtained a large genome-wide sample of informative orthologous UCE markers, insufficient phylogenetic signal and paralogy can also be ruled out (e.g. Funk and Omland, 2003). Given that we rejected a phylogenetic network allowing reticulations due to episodic introgression between species/lineages (see Section 3.4), the evidence for hybridization-mediated introgression is also weak. Sampling of additional individuals nearby is needed to test this pattern of paraphyly, which may reflect unsorted ancestral polymorphism (ILS) retained due to the on-average moderate to large population sizes of *Anoura* lineages during the past ~ 2 Myr (Supplementary Table S3; Figs. 5 and S3). Alternatively, this individual may be part of a subpopulation of *A. cultrata* that has lost the blade-tooth and other diagnostic characteristics of the species.

4.2. Divergence times and historical biogeography of Anoura

Our results contribute to our understanding of Andean biogeography by providing a new perspective on the historical deployment of *Anoura* species/lineage across changing Neotropical landscapes of the past ~ 9 Myr since the late Miocene (Tortonian). Although the Andes began to form from 30 to 20 Ma, tectonic uplift accelerated to generate the majority of modern elevations in the Northern Andes during the last ~ 10 Myr (Gregory-Wodzicki, 2000; Garzione et al., 2008; Hoorn et al., 2010; Mora et al., 2010; Garzione et al., 2014). Our results suggest that the ancestral *Anoura* stock initially evolved during this period of accelerated Andean uplift, with much of the diversification of the extant species/lineages occurring after ~ 4 Ma in the Pliocene (Fig. 5). These results place the diversification of *Anoura* contemporaneously with that other species of nectarivorous bats within the subfamily Glossophaginae (Rojas et al., 2016) but suggest that *Anoura* evolved with a faster speciation rate (or lower extinction rate), leaving *Anoura* as the most speciose extant genus of glossophagines (Cirranello and Simmons, 2020; Calderón-Acevedo et al., 2021). However, *Anoura* has apparently diversified at a slower rate relative to genera within other phyllostomid subfamilies such as the Stenodermatinae, which is the most speciose subfamily within the family Phyllostomidae (Velazco and Patterson, 2008; Velazco and Simmons, 2011; Velazco and Patterson, 2013; Rojas et al., 2016; Cirranello and Simmons, 2020).

Our best-supported ancestral area reconstruction provides a historical biogeographical scenario yielding several novel insights into how *Anoura* species/lineages might have attained their present-day geographical distributions across the Neotropics (Fig. 6). First, we infer that the ancestral *Anoura* lineage had a wide geographical distribution spanning South America, which fragmented over time into the four major lineages in our phylogeny. Second, and consistent with our initial expectations, parapatric speciation patterns predominate in our BioGeoBEARS reconstructions, with limited evidence for clear patterns of allopatric speciation due to vicariance at prominent geographical barriers. This is perhaps unsurprising, given that most species within the genus have broadly sympatric modern ranges, and there are localities today in which 5 or more species can be identified (Handley, 1960, 1976, 1984; Alberico et al., 2000; Pacheco et al., 2018). However, we cannot rule out the possibility that the initial divergences of major lineages and species of *Anoura* occurred in an allopatric context, and then species more recently expanded their range to assume overlapping positions, e.g. during climatic fluctuations of the mid-late Pleistocene. Paleoclimatic modeling analyses inferring the past geographical range dynamics of *Anoura* species/lineages are needed to assess this possibility further. We also find evidence for several mid-crown to recent speciation events that must have occurred within the distributions of the ancestors of the more wide-ranging *Anoura* species, *A. caudifer* and *A. geoffroyi*. For example, the divergence of *A. fistulata* from the MRCA of *A. cadenai* + *A.* sp. A, as well as the divergence between the latter two species, all likely occurred within the Andes Mountains, a region where present-day distributions of *A. caudifer* and *A. geoffroyi* both overlap (Fig. 1; Mantilla-Meluk and Baker, 2006, 2010). Third, our historical biogeographical

reconstruction for *Anoura* suggests that areas of marked topographic relief, including Andean mountain ranges and inter-Andean valleys, as well as features of the Amazon Basin (e.g. riverine barriers), appear not to have limited gene flow sufficiently to promote allopatric speciation in *Anoura*.

It remains unclear which ecological or genetic mechanisms have been at play in maintaining the distinctiveness of *Anoura* species despite apparently long periods of time with sympatric distributions, as indicated by our BioGeoBEARS results, and this suggests several intriguing avenues for future research (with the caveat being, as per above, that distributions of the incipient lineages may have originally been allopatric). Future studies would do well to consider factors potentially influencing speciation and/or maintenance of species boundaries in *Anoura* by combining information from paleoclimatic modeling and distributional hindcasting, phylogenomics, historical demography, behavior, and bioacoustics (e.g. echolocation).

4.3. Taxonomic implications

Our findings have several important taxonomic implications for *Anoura* and help to clarify the identity and limits of several species within the genus. First, the type and paratype specimens of "*A. carishina*" are polyphyletic and nested within the *A. latidens* clade with definitive support (Fig. 3). This strongly supports the conclusions of previous work based on integrating perspectives from morphometrics and phylogenomics, which concluded that "*A. carishina*" should be treated as a junior synonym of *A. latidens* (Calderón-Acevedo, 2019; Calderón-Acevedo et al., 2021). In line with the finding that one paratype (Acar115) corresponds morphologically to *A. geoffroyi* (Calderón-Acevedo et al., 2021), this same specimen was also inferred herein as nesting within a clade of *A. geoffroyi* specimens with definitive support. Second, the interdigitated pattern of *A. caudifer* specimens and specimens previously attributed to *A. aequatoris* supports the monotypic status of *A. caudifer* and strongly supports *A. aequatoris* sensu Mantilla-Meluk and Baker (2006) as being considered a synonym of *A. caudifer* (also see Griffiths and Gardner, 2008; Jarrín-V. and Kunz, 2008; Calderón-Acevedo, 2019). Finally, we find that the Peruvian samples of *A. geoffroyi* analyzed herein (Aperu69, Aperu269, Aperu270, Aperu274), which were previously ascribed to *A. peruana* (Mantilla-Meluk and Baker, 2010), interdigitate with Andean and Caribbean samples of *A. geoffroyi* (Fig. 3; Supplementary Tables S1 and S2). This supports previous morphological work suggesting that the traits used to separate *A. peruana* from *A. geoffroyi* are not reliable as diagnostic characters (Calderón-Acevedo, 2019; Calderón-Acevedo et al., 2021), and supports the synonymization of *A. peruana* within *A. geoffroyi*. To better understand the taxonomy of *A. geoffroyi*, such as the interdigitated pattern we detected for individuals from northern and central Andean populations, we recommend further phylogeographic studies with an expanded sample size.

Our results also corroborate previous morphology-based findings regarding the monophyly of small-bodied *Anoura* species. Specifically, Pacheco et al. (2018) suggested that several traits shared by taxa in the small-bodied *A. caudifer* species complex, including *A. aequatoris*, *A. cadenai*, *A. caudifer*, *A. fistulata*, *A. luismanueli*, and the newly-described *A. javieri*, may represent synapomorphies for this group, and that ipso facto the generic name *Lonchoglossa* could be used to refer to this group. Although *A. javieri* is not represented in our phylogeny, our results suggest that the other taxa in the *A. caudifer* species complex do indeed form a monophyletic group, and thus they support the use of *Lonchoglossa* for this clade. Still, we suggest that this should be applied as a subgenus rank, rather than elevating the clade to the genus level. This would limit nomenclatural and taxonomic instability while still allowing mammologists to refer to a monophyletic taxonomic group that is governed by the International Code of Zoological Nomenclature (Teta, 2019). Also, using *Lonchoglossa* as a generic name for the *A. caudifer* species complex would imply that *A. cultrata* should receive a new generic name, with *A. geoffroyi* and *A. latidens* remaining under the genus *Anoura*. Uncertainty as to the phylogenetic placement of *A. cultrata* among our results further supports retaining the genus-rank name of *Anoura* for all current species, and applying *Lonchoglossa* as a subgenus comprised of the species *A. caudifer*, *A. luismanueli*, *A. cadenai*, *A. fistulata*, *A.* sp. A, and *A. javieri*.

5. Conclusions

Our study presents the most comprehensive phylogenetic perspective on the evolution of *Anoura* to date, based on analyses of thousands of genome-wide UCEs and extensive (~88%) taxon sampling of the genus. Our results infer the phylogeny of *Anoura*, help to resolve several taxonomic issues, and lend credence to the use of the name *Lonchoglossa* as a subgenus rank when referring to the small-bodied *Anoura* species in the *A. caudifer* species complex (sensu Mantilla-Meluk and Baker, 2006). The best-supported historical biogeographical scenario for the genus suggests that modern-day *Anoura* evolved since the Miocene through the progressive fragmentation of a wide-ranging ancestral *Anoura* lineage, involving Plio–Pleistocene diversification of multiple geographically overlapping clades, with only a small number of allopatric speciation patterns clearly consistent with vicariance events; however, uncertainty of these inferences was great at deeper internal nodes. By shedding light on the tempo, mode, and geographic context of *Anoura* evolution, our study adds to a growing literature on Andean biogeography and systematics (e.g. Morales-Martínez et al., 2021; Rodríguez-Posada et al., 2021) helping to understand the mechanisms generating high species diversity and endemism in what is a biodiversity hotspot not only for bats, but across terrestrial species assemblages (e.g. Meyers et al. 2000).

We recommend four avenues of future research to further elucidate *Anoura* evolution. These include (1) additional sampling within and among species, including improved geographical and numerical sampling of *A. luismanueli* and *A. geoffroyi*, and the addition of specimens from *A. javieri*; (2) testing hypotheses about the ancestral geographical range dynamics of *Anoura* lineages using paleoclimatic modeling approaches (e.g. hindcasting) that take into account the effect of glaciation periods on environmental-climatic variation; (3) species delimitation studies integrating multiple data types and analytical frameworks; and (4) studies focused on differences in ecology, echolocation, and mate choice between *Anoura* species in order to improve our understanding of mechanisms defining and maintaining species boundaries in these morphologically similar but wonderfully genetically differentiated species.

Funding statement

This work was supported by the Whitney Harris Center for World Ecology at the University of Missouri–St. Louis, by the Biology Graduate Student Association at the University of Missouri-St. Louis, and by an equipment grant from Idea Wild. Additionally, JCB received stipend support during this project from U.S. National Science Foundation grant DEB-1754802 to NM.

CRediT authorship contribution statement

Camilo A. Calderón-Acevedo: Conceptualization, Funding acquisition, Data curation, Formal analysis, Investigation, Methodology, Validation, Visualization, Writing – original draft. **Justin C. Bagley:** Conceptualization, Data curation, Formal analysis, Investigation, Methodology, Supervision, Software, Validation, Visualization, Writing – original draft. **Nathan Muchhala:** Conceptualization, Funding acquisition, Investigation, Project administration, Methodology, Supervision, Writing – review & editing.

Declaration of Competing Interest

The authors declare that they have no known competing financial interests or personal relationships that could have appeared to influence the work reported in this paper.

Data accessibility

Raw sequence data are deposited in the NCBI Sequence Read Archive database (BioProject PRJNA529738). Supplementary figures and data associated with this article, including supplementary files below (in Appendix A) as well as aligned sequences, trees, and input files, are available in the accompanying Mendeley Data accession located at: <http://dx.doi.org/10.17632/xhxbf5hyyt.1>.

Acknowledgements

For their assistance, including access to specimens or tissue samples as well as internal databases, we thank the curators and other colleagues from several mammalogical collections that were visited during the course of this project. Specifically, we wish to thank H. López-Arévalo, M. Rodríguez-Posada, C. Cárdenas and D. Morales-Martínez (ICN), D. Zurc (CSJ), S. Solari (CTUA), B. Patterson (FMNH), and T. Lee (ACUNHC) for providing tissue samples. We also are grateful to J. F. Díaz-Nieto, M. Londoño-Gaviria and J. M. Martínez-Cerón and S. Solari for assistance with fieldwork for this project, as well as helpful discussions on the species limits of *Anoura*. JCB wishes to thank the Virginia Commonwealth University Center for High Performance Computing (CHiPC) for access to generous supercomputing resources used during analyses. CAC wishes to thank R.E. Acevedo-C and J. Calderón-G for their support.

Appendix A. Supplementary material

Supplementary data to this article may be found in the enclosed Appendix A. Supplementary material file (PDF).

Supplementary data to this article can be found online at https://doi.org/10.1016/j.ympev.2021.107356.

References

Akaike, H., 1974. A new look at the statistical model identification. IEEE Trans. Automat. Contr. 19, 716–723.

Alberico, M., Cadena, A., Hernández-Camacho, J., Muñoz-Saba, Y., 2000. Mamíferos (Synapsida: Theria) de Colombia. Biota Colombiana 1, 43–75.

Allen, H., 1898. On the Glossophaginae. T. Am. Philos. Soc. 19, 237–266.

Andermann, T., Fernandes, A.M., Olsson, U., Töpel, M., Pfeil, B., Oxelman, B., Aleixo, A., Faircloth, B.C., Antonelli, A., 2019. Allele phasing greatly improves the phylogenetic utility of ultraconserved elements. Syst. Biol. 68, 32–46. https://doi.org/10.1093/sysbio/syy039.

Angelis, K., dos Reis, M., 2015. The impact of ancestral population size and incomplete lineage sorting on Bayesian estimation of species divergence times. Curr. Zool 61, 874–885. https://doi.org/10.1093/czoolo/61.5.874.

Bagley, J.C., 2019a. MAGNET v1.1.0. GitHub repository. Available at: <https://github.com/justincbagley/MAGNET>.

Bagley, J.C., 2019. PIrANHA v0.3a2. GitHub repository. Available at: <https://github.com/justincbagley/piranha>.

Bagley, J.C., 2019. PIrANHA v0.4a3. GitHub repository. Available at: <https://github.com/justincbagley/piranha>.

Bagley, J.C., Uribe-Convers, S., Carlsen, M.M., Muchhala, N., 2020. Utility of targeted sequence capture for phylogenomics in rapid, recent angiosperm radiations: Neotropical *Burmeistera* bellflowers as a case study. Mol. Phylogenet. Evol. 152, 106769 https://doi.org/10.1016/j.ympev.2020.106769.

Baker, R.J., Hood, C.S., Honeycutt, R.L., 1989. Phylogenetic relationships and classification of the higher categories of the New World bat family Phyllostomidae. Syst. Biol. 38, 228–238. https://doi.org/10.2307/2992284.

Baker, R.J., Hoofer, S.R., Porter, C.A., Van Den Bussche, R.A., 2003. Diversification among New World leaf-nosed bats: an evolutionary hypothesis and classification inferred from digenomic congruence of DNA sequence. Occasional Papers, Museum of Texas Tech University 230, 1–32.

Bilderbeek, R.J., Etienne, R.S., 2018. babette: BEAUti 2, BEAST2 and Tracer for R. bioRxiv, 271866.

Blair, C., Bryson Jr., R.W., Linkem, C.W., Lazcano, D., Klicka, J., McCormack, J.E., 2019. Cryptic diversity in the Mexican highlands: thousands of UCE loci help illuminate phylogenetic relationships, species limits and divergence times of montane rattlesnakes (Viperidae: *Crotalus*). Mol. Ecol. Res. 19, 349–365. https://doi.org/10.1111/1755-0998.12970.

Burnham, K.P., Anderson, D.R., 2002. Model Selection and Multimodel Inference: A Practical Information-Theoretic Approach, 2nd Ed. Springer-Verlag, New York.

Burnham, K.P., Anderson, D.R., 2004. Multimodel inference: understanding AIC and BIC in Model Selection. Sociol. Method. Res. 33, 261–304. https://doi.org/10.1177/0049124104268644.

Cabrera, A., 1958. Catálogo de los Mamíferos de América del Sur. Rev. Mus. Argentino de Cienc. Nat. "Bernardino Rivadavia" 4, 1–307.

Calderón-Acevedo, C.A., 2019. Taxonomy, Species Limits, and Phylogenetic Relationships of Anoura Gray 1838 (Chiroptera: Phyllostomidae). Doctoral dissertation, University of Missouri-St. Louis, St. Louis, MO. Available at: https://irl.umsl.edu/dissertation/888.

Calderón-Acevedo, C.A., Muchhala, N., 2018. Identification and diagnosis of *Anoura fistulata* with remarks on its presumed presence in Bolivia. J. Mammal. 99, 131–137. https://doi.org/10.1093/jmammal/gyx159.

Calderón-Acevedo, C.A., Muchhala, N., 2020. First report of the Broad-toothed Tailless Bat, Anoura latidens Handley, 1984 (Chiroptera, Phyllostomidae), in Bolivia. Check List 16, 1545–1550. https://doi.org/10.15560/16.6.1545.

Calderón-Acevedo, C.A., Rodríguez-Posada, M.E., Muchhala, N., 2021. Morphology and genetics concur that *Anoura carishina* is a synonym of *Anoura latidens* (Chiroptera, Glossophaginae). Mammalia. 85, 471–481. https://doi.org/10.1515/mammalia-2020-0183.

Carstens, B.C., Lundrigan, B.L., Myers, P., 2002. A phylogeny of the neotropical nectar-feeding bats (Chiroptera: Phyllostomidae) based on morphological and molecular data. J. Mamm. Evol. 9, 23–53. https://doi.org/10.1023/A:1021331711108.

Chifman, J., Kubatko, L., 2014. Quartet inference from SNP data under the coalescent model. Bioinformatics 30, 3317–3324. https://doi.org/10.1093/bioinformatics/btu530.

Chifman, J., Kubatko, L., 2015. Identifiability of the unrooted species tree topology under the coalescent model with time-reversible substitution processes, site-specific rate variation, and invariable sites. J. Theor. Biol. 374, 35–47. https://doi.org/10.1016/j.jtbi.2015.03.006.

Cirranello, A.L., Simmons, N.B., 2020. 4. Diversity and discovery: a Golden Age. In: Fleming, T.H., Dávalos, L.M., Mello, M.A.R. (Eds.), Phyllostomid Bats: A Unique Mammalian Radiation. University of Chicago Press, Chicago, pp. 43–62.

Datzmann, T., von Helversen, O., Mayer, F., 2010. Evolution of nectarivory in phyllostomid bats (Phyllostomidae Gray, 1825, Chiroptera: Mammalia). BMC Evol. Biol. 10, 165. https://doi.org/10.1186/1471-2148-10-165.

Dávalos, L.M., Velazco, P.M., Warsi, O.M., Smits, P.D., Simmons, N.B., 2014. Integrating incomplete fossils by isolating conflicting signal in saturated and non-independent morphological characters. Syst. Biol. 63, 582–600. https://doi.org/10.1093/sysbio/syu022.

de Moraes Weber, M., Viveiros Grelle, C.E., 2012. Does environmental suitability explain the relative abundance of the tailed tailless bat, *Anoura caudifer*? Nat. Conservaçao 10, 221–227. https://doi.org/10.4322/natcon.2012.035.

Del Fabbro, C., Scalabrin, S., Morgante, M., Giorgi, F.M., 2013. An extensive evaluation of read trimming effects on Illumina NGS data analysis. PLoS One 8, e85024. https://doi.org/10.1371/journal.pone.0085024.

Díaz, M.M., Solari, S., Aguirre, L.F., Aguiar, L.M.S., Barquez, R.M., 2016. Clave de identificación de los murciélagos de Sudamérica. Publicación Especial. PCMA (Programa de Conservación de los Murciélagos de Argentina) 2, 1–160.

dos Reis, M., 2020. bppr: An R package for BPP. R package version 0.6.1. Available at: <https://github.com/dosreislab/bppr>.

Esselstyn, J.A., Oliveros, C.H., Swanson, M.T., Faircloth, B.C., 2017. Investigating difficult nodes in the placental mammal tree with expanded taxon sampling and thousands of ultraconserved elements. Genome Biol. Evol. 9, 2308–2321. https://doi.org/10.1093/gbe/evx168.

Faircloth, B.C., 2013. Illumiprocessor: a Trimmomatic wrapper for parallel adapter and quality trimming. See 2016. https://doi.org/10.6079/J9ILL (accessed 4 November.

Faircloth, B.C., 2016. PHYLUCE is a software package for the analysis of conserved genomic loci. Bioinformatics 32, 786–788. https://doi.org/10.1093/bioinformatics/btv646.

Faircloth, B.C., 2017. Identifying conserved genomic elements and designing universal bait sets to enrich them. Method. Ecol. Evol. 8, 1103–1112. https://doi.org/10.1111/2041-210X.12754.

Faircloth, B.C., McCormack, J.E., Crawford, N.G., Harvey, M.G., Brumfield, R.T., Glenn, T.C., 2012. Ultraconserved elements anchor thousands of genetic markers spanning multiple evolutionary timescales. Syst. Biol. 61, 717–726. https://doi.org/10.1093/sysbio/sys004.

Felsenstein, J., 1978. Cases in which parsimony or compatibility methods will be positively misleading. Syst. Biol. 27, 401–410. https://doi.org/10.1093/sysbio/27.4.401.

Flouri, T., Jiao, X., Rannala, B., Yang, Z., 2018. Species tree inference with BPP using genomic sequences and the multispecies coalescent. Mol. Biol. Evol. 35 (10), 2585–2593. https://doi.org/10.1093/molbev/msy147.

Flouri, T., Jiao, X., Rannala, B., Yang, Z., 2020. A Bayesian implementation of the multispecies coalescent model with introgression for phylogenomic analysis. Mol. Biol. Evol. 37 (4), 1211–1223. https://doi.org/10.1093/molbev/msz296.

Funk, D.J., Omland, K.E., 2003. Species-level paraphyly and polyphyly: frequency, causes, and consequences, with insights from animal mitochondrial DNA. Ann. Rev. Ecol. Evol. Syst. 34 (1), 397–423. https://doi.org/10.1146/annurev.ecolsys.34.011802.132421.

Galindo-Galindo, C., Castro-Campillo, A., Salame-Méndez, A., Ramírez-Pulido, J., 2000. Reproductive events and social organization in a colony of *Anoura geoffroyi* (Chiroptera: Phyllostomidae) from a temperate Mexican cave. Acta Zool. Mex. 80, 51–68.

Garzione, C.N., Auerbach, D.J., Smith, J.-J.-S., Rosario, J.J., Passey, B.H., Jordan, T.E., Eiler, J.M., 2014. Clumped isotope evidence for diachronous surface cooling of the

Altiplano and pulsed surface uplift of the Central Andes. Earth Planet. Sc. Lett. 393, 173–181. https://doi.org/10.1016/j.epsl.2014.02.029.
Garzione, C.N., Hoke, G.D., Libarkin, J.C., Withers, S., MacFadden, B., Eiler, J., Ghosh, P., Mulch, A., 2008. Rise of the Andes. Science 320, 1304–1307. https://doi.org/10.1126/science.1148615.
Giarla, T.C., Esselstyn, J.A., 2015. The challenges of resolving a rapid, recent radiation: empirical and simulated phylogenomics of philippine shrews. Syst. Biol. 64, 727–740. https://doi.org/10.1093/sysbio/syv029.
Gray, J., 1838. A revision of the genera of bats (Vespertilionidae), and the description of some new genera and species. Magazine of Zoology and Botany 2, 483–505.
Gregory-Wodzicki, K.M., 2000. Uplift history of the Central and Northern Andes: a review. Geol. Soc. Am. Bull. 112, 1091–1105.
Griffiths, T.A., 1982. Systematics of the New World nectar-feeding bats (Mammalia, Phyllostomidae), based on the morphology of the hyoid and lingual regions. Am. Mus. Novit. 2742, 1–45.
Griffiths, T.A., Gardner, A.L., 2008. Subfamily Glossophaginae Bonaparte, 1845. In: Gardner, A. (Ed.), Mammals of South America, Vol 1. Marsupials, Xenarthrans, Shrews, and Bats. Chicago: The University of Chicago Press, pp. 224–244.
Handley Jr., C.O., 1960. Description of New Bats from Panama. Smithsonian Institution, Washington, D.C.
Handley Jr., C.O., 1976. Mammals of the Smithsonian Venezuelan project. Brigham Young University Science Bulletin-Biological Series 20, 1–91.
Handley Jr., C.O., 1984. New species of mammals from northern South America: a long-tongued bat, genus *Anoura* Gray. Proc. Biol. Soc. Wash. 97, 513–521.
Hoorn, C., Wesselingh, F., Ter Steege, H., Bermudez, M., Mora, A., Sevink, J., Sanmartín, I., Sanchez-Meseguer, A., Anderson, C., Figueiredo, J., 2010. Amazonia through time: Andean uplift, climate change, landscape evolution, and biodiversity. Science 330, 927–931. https://doi.org/10.1126/science.1194585.
Hosner, P.A., Faircloth, B.C., Glenn, T.C., Braun, E.L., Kimball, R.T., 2016. Avoiding missing data biases in phylogenomic inference: an empirical study in the landfowl (Aves: Galliformes). Mol. Biol. Evol. 33 (4), 1110–1125. https://doi.org/10.1093/molbev/msv347.
Husson, A.M., 1962. The bats of Suriname. Zool. Verhandelingen 58, 1–278.
Jarrín-V., P., Coello, D., 2012. Quantification of morphological variation within species of *Anoura* from Ecuador, with an emphasis on *A. fistulata* (Chiroptera: Phyllostomidae). Acta Chiropterol. 14, 317–333. https://doi.org/10.3161/150811012X661648.
Jarrín-V., P., Kunz, T.H., 2008. Taxonomic history of the genus *Anoura* (Chiroptera: Phyllostomidae) with insights into the challenges of morphological species delimitation. Acta Chiropterol. 10, 257–269. https://doi.org/10.3161/150811008X414836.
Katoh, K., Standley, D.M., 2013. MAFFT multiple sequence alignment software version 7: improvements in performance and usability. Mol. Biol. Evol. 30, 772–780. https://doi.org/10.1093/molbev/mst010.
Kumar, S., Filipski, A.J., Battistuzzi, F.U., Kosakovsky Pond, S.L., Tamura, K., 2012. Statistics and truth in phylogenomics. Mol. Biol. Evol. 29, 457–472. https://doi.org/10.1093/molbev/msr202.
Landis, M.J., Matzke, N.J., Moore, B.R., Huelsenbeck, J.P., 2013. Bayesian analysis of biogeography when the number of areas is large. Syst. Biol. 62, 789–804. https://doi.org/10.1093/sysbio/syt040.
Lanfear, R., Calcott, B., Kainer, D., Mayer, C., Stamatakis, A., 2014. Selecting optimal partitioning schemes for phylogenomic datasets. BMC Evol. Biol. 14, 82. https://doi.org/10.1186/1471-2148-14-82.
Lanfear, R., Frandsen, P.B., Wright, A.M., Senfeld, T., Calcott, B., 2017. PartitionFinder 2: new methods for selecting partitioned models of evolution for molecular and morphological phylogenetic analyses. Mol. Biol. Evol. 34, 772–773. https://doi.org/10.1093/molbev/msw260.
Lohse, M., Bolger, A.M., Nagel, A., Fernie, A.R., Lunn, J.E., Stitt, M., Usadel, B., 2012. *RobiNA*: a user-friendly, integrated software solution for RNA-Seq-based transcriptomics. Nucleic Acids Res. 40, W622–W627. https://doi.org/10.1093/nar/gks540.
Mantilla-Meluk, H., Baker, R.J., 2006. Systematics of small *Anoura* (Chiroptera: Phyllostomidae) from Colombia, with description of a new species. Occasional Papers, Museum of Texas Tech University 261, 1–18.
Mantilla-Meluk, H., Baker, R.J., 2010. New species of *Anoura* (Chiroptera: Phyllostomidae) from Colombia, with systematic remarks and notes on the distribution of the *A. geoffroyi* complex. Occasional Papers, Museum of Texas Tech University 292, 1–19.
Mantilla-Meluk, H., Jiménez-Ortega, A.M., Baker, R.J., 2009. Range Extension of *Anoura aequatoris* and notes on distributional limits of small *Anoura* in Colombia. Revista Institucional Universidad Tecnológica del Chocó Investigación Biodiversidad y Desarrollo 28, 107–112.
Matzke, N.J., 2013a. BioGeoBEARS: BioGeography with Bayesian (and likelihood) Evolutionary Analysis in R scripts. R package, version 0.2. 1, published July 27, 2013. Available at: <http://phylo.wikidot.com/biogeobears>.
Matzke, N.J., 2013. Probabilistic historical biogeography: new models for founder-event speciation, imperfect detection, and fossils allow improved accuracy and model-testing. Front. Biogeogr. 5, 242–248.
McCormack, J.E., Faircloth, B.C., Crawford, N.G., Gowaty, P.A., Brumfield, R.T., Glenn, T.C., 2012. Ultraconserved elements are novel phylogenomic markers that resolve placental mammal phylogeny when combined with species-tree analysis. Genome Res. 22, 746–754. https://doi.org/10.1101/gr.125864.111.
Mirarab, S., Reaz, R., Bayzid, M.S., Zimmermann, T., Swenson, M.S., Warnow, T., 2014. ASTRAL: genome-scale coalescent-based species tree estimation. Bioinformatics 30, i541–i548. https://doi.org/10.1093/bioinformatics/btu462.
Mirarab, S., Warnow, T., 2015. ASTRAL-II: coalescent-based species tree estimation with many hundreds of taxa and thousands of genes. Bioinformatics 31 (12), i44–i52. https://doi.org/10.1093/bioinformatics/btv234.
Mora, A., Baby, P., Roddaz, M., Parra, M., Brusset, S., Hermoza, W., Espurt, N., 2010. Tectonic history of the Andes and sub-Andean zones: implications for the development of the Amazon drainage basin. In: Hoorn, C., Wesselingh, F.P. (Eds.), Amazonia: Landscape and Species Evolution. Blackwell Publishing Ltd, pp. 38–60.
Morales, A.E., Jackson, N.D., Dewey, T.A., O'Meara, B.C., Carstens, B.C., 2017. Speciation with gene flow in North American *Myotis* bats. Syst. Biol. 66, 440–452. https://doi.org/10.1093/sysbio/syw100.
Morales-Martínez, D.M., Rodríguez-Posada, M.E., Ramírez-Chaves, H.E., 2021. A new cryptic species of yellow-eared bat *Vampyressa melissa* species complex (Chiroptera: Phyllostomidae) from Colombia. J. Mammal. 102, 90–100. https://doi.org/10.1093/jmammal/gyaa137.
Muchhala, N., 2006. Nectar bat stows huge tongue in its rib cage. Nature 444, 701–702. https://doi.org/10.1038/444701a.
Muchhala, N., Jarrín-V., P., 2002. Flower visitation by bats in cloud forests of Western Ecuador. Biotropica 34(3), 387–395. https://doi.org/10.1111/j.1744-7429.2002.tb00552.x.
Muchhala, N., Mena, V.P., Albuja, V.L., 2005. A new species of *Anoura* (Chiroptera: Phyllostomidae) from the Ecuadorian Andes. J. Mammal. 86 (3), 457–461. https://doi.org/10.1644/1545-1542(2005)86[457:ANSOAC]2.0.CO;2.
Muchhala, N., Thomson, J.D., 2009. Going to great lengths: selection for long corolla tubes in an extremely specialized bat–flower mutualism. Proc. R. Soc. B. 276 (1665), 2147–2152. https://doi.org/10.1098/rspb.2009.0102.
Myers, N., Mittermeier, R.A., Mittermeier, C.G., da Fonseca, G.A.B., Kent, J., 2000. Biodiversity hotspots for conservation priorities. Nature 403, 853–858. https://doi.org/10.1038/35002501.
Nagorsen, D., Tamsitt, J.R., 1981. Systematics of *Anoura cultrata*, *A. brevirostrum*, and *A. werckleae*. J. Mammal. 62, 82–100.
Olave, M., Meyer, A., 2020. Implementing large genomic SNP datasets in phylogenetic network reconstructions: a case study of particularly rapid radiations of cichlid fish. Syst. Biol. 69 (5), 848–862. https://doi.org/10.1093/sysbio/syaa005.
Pacheco, V., Sánchez-Vendizú, P., Solari, S., 2018. A new species of *Anoura* Gray, 1838 (Chiroptera: Phyllostomidae) from Peru, with taxonomic and biogeographic comments on species of the *Anoura caudifer* complex. Acta Chiropterol. 20, 31–50. https://doi.org/10.3161/15081109ACC2018.20.1.002.
Peters, W., 1868. Über die zu den Glossophagae gehörigen Flederthiere und über eine neue Art der Gattung Coleura. Auszug aus dem Monatsbericht Königlichen Akademie der Wissenschaften zu Berlin 1869, 361–368.
Rannala, B., Yang, Z., 2003. Bayes estimation of species divergence times and ancestral population sizes using DNA sequences from multiple loci. Genetics 164 (4), 1645–1656. https://doi.org/10.1093/genetics/164.4.1645.
Ree, R.H., Smith, S.A., 2008. Maximum likelihood inference of geographic range evolution by dispersal, local extinction, and cladogenesis. Syst. Biol. 57, 4–14. https://doi.org/10.1080/10635150701883881.
Roch, S., Steel, M., 2015. Likelihood-based tree reconstruction on a concatenation of aligned sequence data sets can be statistically inconsistent. Theor. Popul. Biol. 100, 56–62. https://doi.org/10.1016/j.tpb.2014.12.005.
Rodríguez-Posada, M.E., Morales-Martínez, D.M., Ramírez-Chaves, H.E., Martínez-Medina, D., Calderón-Acevedo, C.A., 2021. A new species of Long-eared Brown Bat of the genus *Histiotus* (Chiroptera) and the revalidation of *Histiotus colombiae*. Caldasia 43, 221–234. https://doi.org/10.15446/caldasia.v43n2.85424.
Rojas, D., Moreira, M., Ramos Pereira, M.J., Fonseca, C., Dávalos, L.M., 2018. Updated distribution maps for neotropical bats in the superfamily Noctilionoidea. Ecology 99, 2131–2131. https://doi.org/10.1002/ecy.2404.
Rojas, D., Vale, Á., Ferrero, V., Navarro, L., 2012. The role of frugivory in the diversification of bats in the Neotropics. J. Biogeogr. 39, 1948–1960. https://doi.org/10.1111/j.1365-2699.2012.02709.x.
Rojas, D., Warsi, O.M., Dávalos, L.M., 2016. Bats (Chiroptera: Noctilionoidea) challenge a recent origin of extant neotropical diversity. Syst. Biol. 65 (3), 432–448. https://doi.org/10.1093/sysbio/syw011.
Ronquist, F., 1997. Dispersal-vicariance analysis: a new approach to the quantification of historical biogeography. Syst. Biol. 46, 195–203.
Sanborn, C.C., 1933. Bats of the genera *Anoura* and *Lonchoglossa*. Zoological Series of the Field Museum of Natural History 20, 23–28.
Sanborn, C.C., 1943. External characters of the bats of the subfamily Glossophaginae. Zoological Series of the Field Museum of Natural History 24, 271–277.
Sanderson, M.J., 2002. Estimating absolute rates of molecular evolution and divergence times: a penalized likelihood approach. Mol. Biol. Evol. 19, 101–109. https://doi.org/10.1093/oxfordjournals.molbev.a003974.
Sayyari, E., Mirarab, S., 2016. Fast coalescent-based computation of local branch support from quartet frequencies. Mol. Biol. Evol. 33, 1654–1668. https://doi.org/10.1093/molbev/msw079.
Simpson, G.G., 1945. The principles of classification and a classification of mammals. Bull. Amer. Mus. Nat. His. 85, 1–350.
Simpson, J.T., Wong, K., Jackman, S.D., Schein, J.E., Jones, S.J., Birol, I., 2009. ABySS: a parallel assembler for short read sequence data. Genome Res., gr. 089532.089108. https://doi.org/10.1101/gr.089532.108.
Smith, S.A., O'Meara, B.C., 2012. treePL: divergence time estimation using penalized likelihood for large phylogenies. Bioinformatics 28, 2689–2690. https://doi.org/10.1093/bioinformatics/bts492.
Solís-Lemus, C., Ané, C., 2016. Inferring phylogenetic networks with maximum pseudolikelihood under incomplete lineage sorting. PLoS Genet. 12 (3), e1005896 https://doi.org/10.1371/journal.pgen.1005896.

Solís-Lemus, C., Bastide, P., Ané, C., 2017. PhyloNetworks: a package for phylogenetic networks. Mol. Biol. Evol. 34 (12), 3292–3298. https://doi.org/10.1093/molbev/msx235.

Solís-Lemus, C., Yang, M., Ané, C., 2016. Inconsistency of species tree methods under gene flow. Syst. Biol. 65 (5), 843–851. https://doi.org/10.1093/sysbio/syw030.

Soriano, P.J., Ruiz, A., Arends, A., 2002. Physiological responses to ambient temperature manipulation by three species of bats from Andean cloud forests. J. Mammal. 83, 445–457. https://doi.org/10.1644/1545-1542(2002)083<0445:PRTATM>2.0.CO;2.

Stamatakis, A., 2014. RAxML version 8: a tool for phylogenetic analysis and post-analysis of large phylogenies. Bioinformatics 30, 1312–1313. https://doi.org/10.1093/bioinformatics/btu033.

Suh, A., 2016. The phylogenomic forest of bird trees contains a hard polytomy at the root of Neoaves. Zool. Scr. 45, 50–62. https://doi.org/10.1111/zsc.12213.

Tamsitt, J.R., Nagorsen, D., 1982. Anoura cultrata. Mammalian Species 1–5.

Tamsitt, J.R., Valdivieso, D., 1966. Taxonomic comments on *Anoura caudifer*, *Artibeus lituratus* and *Molossus molossus*. J. Mammal. 47, 230–238.

Teta, P., 2019. The usage of subgenera in mammalian taxonomy. Mammalia 83 (3), 209–211. https://doi.org/10.1515/mammalia-2018-0059.

Van Dam, M.H., Lam, A.W., Sagata, K., Gewa, B., Laufa, R., Balke, M., Faircloth, B.C., Riedel, A., 2017. Ultraconserved elements (UCEs) resolve the phylogeny of Australasian smurf-weevils. PLoS One 12, e0188044. https://doi.org/10.1371/journal.pone.0188044.

Velazco, P.M., Patterson, B.D., 2008. Phylogenetics and biogeography of the broad-nosed bats, genus *Platyrrhinus* (Chiroptera: Phyllostomidae). Mol. Phylogenet. Evol. 49, 749–759. https://doi.org/10.1016/j.ympev.2008.09.015.

Velazco, P.M., Patterson, B.D., 2013. Diversification of the yellow-shouldered bats, genus *Sturnira* (Chiroptera, Phyllostomidae), in the New World tropics. Mol. Phylogenet. Evol. 68, 683–698. https://doi.org/10.1016/j.ympev.2013.04.016.

Velazco, P.M., Simmons, N.B., 2011. Systematics and taxonomy of great striped-faced bats of the genus *Vampyrodes* Thomas, 1900 (Chiroptera: Phyllostomidae). Am. Mus. Novit. 3710, 1–35. https://doi.org/10.1206/3710.2.

Wetterer, A.L., Rockman, M.V., Simmons, N.B., 2000. Phylogeny of phyllostomid bats (Mammalia: Chiroptera): data from diverse morphological systems, sex chromosomes, and restriction sites. Bulletin of the American Museum of Natural history 1–200. https://doi.org/10.1206/0003-0090(2000)248<0001:POPBMC>2.0.CO;2.

Yang, Z., 2015. The BPP program for species tree estimation and species delimitation. Curr. Zool. 61 (5), 854–865. https://doi.org/10.1093/czoolo/61.5.854.

Zhang, C., Rabiee, M., Sayyari, E., Mirarab, S., 2018. ASTRAL-III: polynomial time species tree reconstruction from partially resolved gene trees. BMC Bioinforma. 19 (Suppl. 6), 153. https://doi.org/10.1186/s12859-018-2129-y.